Chemical Geology 269 (2010) 220–236

Contents lists available at ScienceDirect

Chemical Geology

journal homepage: www.elsevier.com/locate/chemgeo

Geochemistry and provenance of stream sediments of the Ganga River and its major tributaries in the Himalayan region, India

Pramod Singh *

Department of Earth Sciences, School of Physical, Chemical and Applied Sciences, Pondicherry University, Pondicherry-605014, India

ARTICLE INFO

Article history:
Received 12 January 2009
Received in revised form 22 September 2009
Accepted 28 September 2009

Editor: R.L. Rudnick

Keywords:
Ganga
Himalayan
Sediment geochemistry
Provenance
Weathering
Climate

ABSTRACT

Major, trace and REE compositions of sediments from the upper Ganga River and its tributaries in the Himalaya have been examined to study the weathering in the Himalayan catchment region and to determine the dominant source rocks to the sediments in the Plains. The Ganga River rises in the Higher Himalaya from the Higher Himalayan Crystalline Series (HHCS) bedrocks and traverses over the Lesser Himalayan Series (LHS) and the Himalayan foreland basin (Siwaliks) rocks before entering into the Gangetic Plains. The major element compositions of sediments, reflected in their low CIA values (45.0–54.7), indicate that silicate weathering has not been an important process in the Himalayan catchment region of the Ganga River. Along the entire traverse, from the HHCS through LHS and the Siwaliks, the sediments from the tributaries and the mainstream Ganga River show higher Na_2O, K_2O, CaO and silica. This, and the higher ratios of La/Sc, Th/Sc and lower ratios of Co/Th, suggest that the source rocks are felsic. The fractionated REE patterns and the significant negative Eu anomalies (Eu/Eu* = 0.27–0.53) indicate highly differentiated source. Moreover, the comparison of the sediments with different source rock lithologies from the HHCS and the LHS for their major elements clearly suggests that the HHCS rocks were the dominant source. Further, comparison of their UCC (upper continental crust) normalized REE patterns suggests that, among the various HHCS rocks, the metasediments (para-gneiss and schist) and Cambro-Ordovician granites have formed the major source rocks. The Bhagirathi and Alaknanda River sediments are dominantly derived from metasediments and those in the Mandakini River from Cambro-Ordovician granites. The resulting composition of the sediments of the Ganga River is due to the mixing of sediments supplied by these tributaries after their confluence at Devprayag. No further change in major, trace and rare earth element compositions of the sediments of the Ganga River after Devprayag up to its exit point to the Plains at Haridwar, suggests little contribution of the Lesser Himalayan and Siwalik rocks to the Ganga River sediments.

© 2009 Elsevier B.V. All rights reserved.

1. Introduction

Chemical weathering of rocks is a major geological process that affects the atmospheric CO_2 concentration, and hence affects global climate (Berner, 1992, 1995; Dupré et al., 2003). At the same time it also affects the nature of sediments produced, and the solute chemistry of rivers, which ultimately controls the ocean water chemistry (Stallard and Edmond, 1983, 1987; Bluth and Kump, 1994; Galy and France-Lanord, 2001). Even though the bedrock is transformed into soil and ultimately into sediments by the combined effects of chemical, biological and physical weathering processes, in response to climate and topography, the original signature of the source still remains preserved in the sediments. The distribution of some trace elements such as Sc, Th, Zr, Cr, Ni Co and REEs, which generally remain immobile during several processes of sediment production, is a useful indicator of source region composition. Thus, sediment geochemistry helps us to decipher the geological evolution of its source region. The sediment chemistry also reflects the nature of weathering at the source, which, in turn, is controlled by climatic and tectonic factors, although there is a strong debate on their dominant influence (Raymo et al., 1988; Drever and Zobrist, 1992; Edmond, 1992; Raymo and Ruddiman, 1992; Derry and France-Lanord, 1996). Thus, in addition to deducing provenance the chemistry of sediments is also a useful indicator of climate and tectonics of the catchment region.

The Ganga River, which drains complex rock types in the Himalaya and passes through diverse climatic and physiographic regions, contributes significantly to the global sediment budget and water discharge to the ocean. The nature of weathering in the Himalaya and its contribution to the solute load are believed to have significant influence over the global climate and ocean water chemistry, particularly after its tectonic upliftment due to the convergence of the Indian and Tibetan plates during the Cenozoic. Thus, it provides immense opportunity to understand the effect of relief, tectonics and

* Tel.: +91 413 2654489.
E-mail address: pramods@yahoo.com.

0009-2541/$ – see front matter © 2009 Elsevier B.V. All rights reserved.
doi:10.1016/j.chemgeo.2009.09.020

climate on the nature of the derivative sediments, and the rate of erosion. The above facts attracted the attention of several workers, who generally relate the chemical and isotopic signature of the solute load of the Ganga River to the nature of chemical weathering in the Himalayan region, and to the change in the ocean water chemistry, particularly during the Cenozoic (Palmer and Edmond, 1989; Vieizer, 1989; Palmer and Edmond, 1992). Raymo and Ruddiman (1992) and Richter et al. (1992) have suggested that the tectonic uplift due to the convergence in the Himalayan region during the Cenozoic could have resulted in increased silicate weathering and elevated $^{87}Sr/^{86}Sr$ ratio of the river water and the ocean since 40 Ma. Since then, the tectonic uplift is also believed to have exerted a strong influence on the chemical budget of some other elements in ocean waters at the global scale (Krishnaswami et al., 1992; Richter et al., 1992; Edmond, 1992; Palmer and Edmond, 1992; Derry and France-Lanord, 1996; Galy et al., 1999). Raymo and Ruddiman (1992) further proposed the theory of global cooling during the Cenozoic as a result of the Himalayan uplift. Their major assumption was that the uplift could have caused enhanced erosion and chemical weathering of the sediments derived from the Himalaya, resulting in an increased rate of CO_2 drawdown (a greenhouse gas), and consequent climate cooling. Since then, the above theory for global cooling has been debated by many researchers. Krishnaswami et al. (1992), Richter et al. (1992), Krishnaswami et al. (1999), Bickle et al. (2003) and Edmond (1992) in their studies have inferred silicate weathering as the dominant source for high $^{87}Sr/^{86}Sr$, whereas Palmer and Edmond (1992), Quade et al. (1997), Harris et al. (1998) and Jacobson et al. (2002) have proposed carbonate weathering as the reason for higher $^{87}Sr/^{86}Sr$. If carbonate weathering had been the source for higher $^{87}Sr/^{86}Sr$ ratio of sea water since the Himalayan uplift, it cannot account for the CO_2 drawdown due to weathering as proposed by Raymo and Ruddiman (1992). Jacobson and Blum (2003) have suggested that the Himalayan and other mountain uplift promote physical weathering by means of glaciation, and not carbon consuming chemical weathering. The debate on the cause of climate change during the Cenozoic calls for further work on the weathering in the Himalaya.

The above inferences on weathering and source of solution input to the Himalayan river water and ultimately to the ocean rely mainly on the chemistry of solute load, and selected carbonate and silicate fractions of the bed load sediments from the Himalayan region, or from the mouth of the river in Bangladesh, or studies carried on few sections from Siwaliks. But none of these studies includes full chemical signature of the detrital sediments. According to an estimate made by Galy and France-Lanord (2001), the total erosion flux from the Himalaya, is double that of the estimate made on the basis of suspended load fluxes in Bangladesh. This implies that the sediments derived by the Himalayan Rivers have variable residence time on land. It is noteworthy that the Himalayan Rivers in general and the Ganga in particular, travel a long distance in the hilly tract and in the Plains before meeting the sea. It also passes through diverse climatic zones, starting from frigid in the upper reaches to warm and humid in the Plains region. Due to higher residence time on land and climatic variation along its tract between hill and the ocean, the sediments may possibly be subjected to changes in addition to those brought by the weathering at their source. These en route changes in sediments may significantly change the solute chemistry of the river waters. Consequently inferences made on the nature of weathering and source of solution input to the ocean, based only on studies of the solute load of the rivers from the Himalayan catchment region, may at times be ambiguous. It is therefore imperative to systematically study the geochemistry of the sediments of these large Himalayan Rivers for the entire stretch from hills to the Plains, to reinterpret the source of the chemical fluxes finally reaching the ocean. In the present study major, trace and rare earth element geochemistry of the sediments collected from the Ganga River and its tributaries, while they pass through different lithological units of the Himalaya, i.e. HHCS, LHS and the Foreland basin deposits (Siwaliks) (Fig. 1), have been examined to evaluate the nature of weathering, sources of sediments in different tributaries, results of mixing of different tributaries and the final output to the river in the Plains. In another study (Singh, 2009) I have reported the chemistry of sediments collected from the different parts of the Ganga Plain, and tried to evaluate the chemical changes brought during their residence in the Plain region as a consequence of different climatic conditions.

2. Geology of the study area

The Himalayan orogeny was a result of Late Cretaceous and early Tertiary (70–40 Ma) collision of the Indian plate with the Eurasian plate. The subduction of Indian plate followed by its collision resulted into series of northward dipping thrust faults, which divided the Himalaya into three tectonic units (Fig. 1) from north to south namely, Higher Himalayan Crystalline Series (HHCS), Lesser Himalayan Series (LHS) and the Siwaliks exposed at different elevations decreasing from north to south. To the North the HHCS is separated from Tethyan strata, which are also known as the Tethyan sedimentary series (TSS), by the Indus–Tsangpo suture zone (ITSZ). The HHCS is made up of high grade late Proterozoic middle and deep crustal metasedimentary rocks (gneisses, schist, quartzites, and metabasics) and biotite ± muscovite granites of Cambro-Ordovician age, with limited carbonate and calcsilicate rocks (Gannser, 1964; Valdiya, 1995). These rocks were subsequently metamorphosed, and later deformed during 500 Ma and Early Miocene between 35 and 20 Ma (Searle et al., 1999). The grade of metamorphism in this series changes from high grade kyanite/sillimanite in the north, to lower-amphibolite and biotite grade in the south. In the north these metasediments, in the Garhwal Himalaya, are intruded by tourmaline + biotite + muscovite ± garnet bearing leucogranites of Miocene/Pliocene age (Searle et al., 1999) that forms high rising plutons (relief > 2000 m) together known as Badrinath–Gangotri granite. The HHCS has the steepest relief, with an average elevation of 4700 m and a range from 1200 m to 7800 m. The southern face of the HHCS is a scarp, 3000–4000 m in elevation (Valdiya, 1980). To the south, the HHCS is separated from another unit, the LHS, by Main Crystalline Thrust/Zone (MCT). The LHS has much lower relief, and an average elevation of 2500 m. The LHS is comprised of Precambrian–Paleozoic pre-Himalayan rocks, metamorphosed to lower grade schist, phyllites, quartzite, calc silicate and variably impure limestone and dolomite (Valdiya, 1995; Johnson and Oliver, 1990). The LHS to its south is delimited by Main Boundary Thrust (MBT), which also forms the northern boundary of Ganges Foreland Basin known as Siwaliks. Siwaliks is comprised of unmetamorphosed sediments deposited in response to the collision, which resulted in rise and erosion of Himalaya.

The Ganga River system is comprised of the Ganga trunk river and its tributaries, the major one being the Bhagirathi, Alaknanda and Mandakini (Fig. 1). The headwater of the Bhagirathi River rises at an altitude of > 4000 m, and Alaknanda River rises at an altitude of ~3500 m from the glaciated valleys of HHCS. Both these tributaries, in this part flow over high grade metasediments, and are surrounded by precipitous cliffs of leucogranites of Mio-Pliocene age that forms high peaks (> 6000 m) with high relief in this part. These two tributaries, then cross various HHCS rocks and enter into the region of LHS rocks before their confluence at Devprayag. These tributaries, in their initial course over HHCS rocks, have very high gradient, e.g. Bhagirathi River in its traverse up to Harsil, descends by > 30 m/km, and Alaknanda River in its initial course up to Joshimath, descends by 30 m/km. Thereafter, gradient of Bhagirathi River between Harsil and Devprayag, in a space of ~200 km, reduces to 10 m/km. In case of Alaknanda River, the gradient further reduces to 3 to 4 m/km between Joshimath and Devprayag. In the HHCS region, after descending from the leucogranite zone, the Bhagirathi River flows over kyanite–

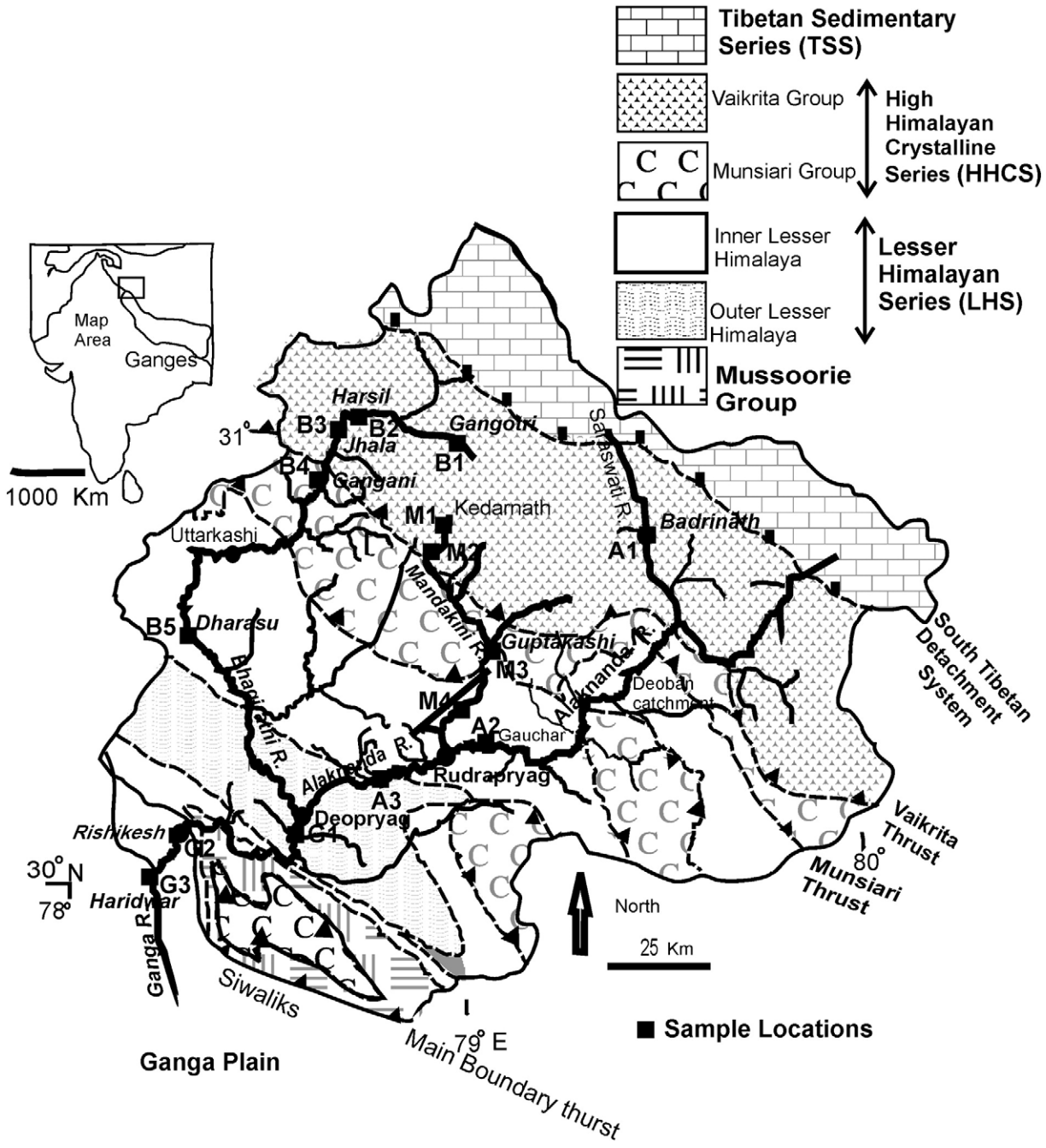

Fig. 1. Geological map of the study area (after Bickle et al., 2001) with sample locations and name.

sillimanite grade metapelites and metaquartzite rocks of Vaikrita group, and thereafter over rocks of Munsiari group comprising of sericite garnet and chlorite schist, granite and augen gneiss, mylonitised porphyritic granite, and small stretches of amphibolite and chlorite schist. After coming out of the HHCS region, the Bhagirathi in the Lesser Himalayan region, flows through quartzarenite and mafic volcanics of Berinag formation, pelites and quartzites of Rautgara formation of Damta group, phyllites and siltstones of the Chandpur formation, again through pelites and quartzites of Chakrata formation of Damta group before meeting Alaknanda River at Deoprayag (Valdiya, 1980). Hereafter the mainstream river is known as the Ganga, which traverse through Chakrata formation, and limestones, dolomite and slates of Krol formation (Mussoorie group), and finally the Siwaliks sediments before entering into the Plains region. Alaknanda River also flows over the similar lithologies, except that, in addition it passes through a 20 km tract of impure dolomite and calcite of Mandhali and Deoban formation. Unlike the above two tributaries, Mandakini originates from the middle part of HHCS, over the high rising peaks of granites. On its descent, it passes through rocks of Vaikrita group and Munsiari group in HHCS transect, and thereafter quartz porphyry, schist's and phyllites of Ramgarh group of LHS before meeting Alaknanda at Rudraprayag, after which, the river carries with the name of Alaknanda.

3. Sampling and analytical methods

River bed load sediments were collected from all the major tributaries of the Ganga River namely Bhagirathi, Alaknanda, Mandakini and after their confluence and from the mainstream Ganga River (Fig. 1). The sediments according to their locations have

Table 1
Major element (in wt.% oxide) and trace element (in ppm) composition of sediments from the Ganga River and its tributaries in the Himalayan catchment region from various locations, along with their CIA, mean size (Mz) in Ø units, various elemental ratios and bulk mineralogical composition.

	Bhagirathi River					Mandakini River				Alaknanda River			The Ganga River		
	(BG Group)					(MG Group)		AMG Group				AG group	(GR Group)		
Sample no.	B1	B2	B3	B4	B5	M1	M2	M3	M4	A2	A3	A1	G1	G2	G3
Latitude (N)	31° 00′ N	31° 2′ 18″ N	31° 01′09″ N	30° 55′ N	30° 05′54″ N	30° 44′ 31″ N	30° 41′ N	30° 30′32″ N	30° 24′ N	30° 16′ 48″ N	30° 13′ 38″ N	30° 44′ 52″ N	30° 7′ 50″ N	30° 07′ 30″ N	29° 58′54″ N
Longitude (E)	78° 55′ E	78° 43′ 37 ″E	78° 42′44″ E	78° 40′ 49″ E	78° 19′17″ E	79° 04′12″ E	79° 3′ E	79° 05′06″ E	79° 2′ E	79° 10′ 15″E	78° 47′ 33″ E	79° 29′ 49″ E	78° 35′ 47″ E	78° 19′ 39″ E	78° 11′ 36″ E
SiO_2	80.09	77.32	78.35	78.34	78.51	74.54	76.54	70.25	73.43	80.65	78.01	77.86	77.66	77.38	78.41
Al_2O_3	10.55	11.65	10.94	11.89	10.23	12.34	11.40	13.73	11.51	9.21	9.27	11.84	9.81	9.87	9.67
TiO_2	0.18	0.31	0.20	0.25	0.31	0.36	0.29	0.55	0.52	0.38	0.36	0.12	0.36	0.31	0.30
FeO	1.44	2.45	1.73	1.87	2.75	3.07	2.41	4.20	5.55	2.44	2.64	1.10	2.68	2.55	2.36
MgO	0.28	0.70	0.71	0.71	1.09	1.18	0.83	1.64	1.22	0.97	1.27	0.34	1.41	1.31	1.34
MnO	0.04	0.04	0.03	0.04	0.04	0.07	0.05	0.06	0.21	0.08	0.08	0.03	0.07	0.07	0.05
CaO	1.49	1.15	1.40	1.37	1.87	2.38	2.04	2.99	2.96	2.19	3.90	1.20	3.24	3.24	3.11
Na_2O	3.29	3.29	3.37	2.66	2.69	2.96	3.17	3.15	2.19	1.62	2.02	3.91	2.28	2.52	2.34
K_2O	2.36	2.88	3.17	2.75	2.44	2.80	3.05	3.20	2.24	2.26	2.28	3.39	2.39	2.58	2.29
P_2O_5	0.29	0.20	0.09	0.13	0.07	0.31	0.23	0.24	0.18	0.20	0.18	0.20	0.12	0.15	0.12
CIA	49.7	52.3	48.7	54.7	49.4	50.2	48.2	49.3	50.2	45.3	49.5	49.0	48.4	46.2	47.9
Mz	1.8	2	2.1	3.0	2.8	2.6	2.8	3.0	1.2	1.5	2.5	2.8	2.6	3.0	2.7
Ba	293	432	398	465	357	653	540	353	448	292	414	296	392	447	406
Sr	85	83	74	79	68	146	114	85	116	66	119	77	101	129	111
Cr	4	19	61	12	10	31	16	86	30	12	12	26	21	73	60
Ni	8	42	20	10	4	17	11	29	13	10	9	12	10	21	19
Sc	5	6		8	7		8			6	10	5		7	
Co	7	8		8	9		9			8	8	7		8	
Th	20	19		15	10		17			13	19	13		12	
U	4	5		5	1		5			4	1	6		1	
Zr	245	254		192	94		210			103	308	127		201	
Y	25	23	19	25	15	28	22	42	46	17	32	20	29	28	24
Al2O3/Na2O	3.2	3.5	3.2	4.5	3.8	4.2	3.6	4.4	5.3	5.7	4.6	3.0	4.3	3.9	4.1
K2O/Na_2O	0.7	0.9	0.9	1.0	0.9	0.9	1.0	1.0	1.0	1.4	1.1	0.9	1.0	1.0	1.0
Na_2O/K_2O	1.4	1.1	1.1	1.0	1.1	1.1	1.0	1.0	1.0	0.7	0.9	1.2	1.0	1.0	1.0
SiO_2/Al_2O_3	7.6	6.6	7.2	6.6	7.7	6.0	6.7	5.1	6.4	8.8	8.4	6.6	7.9	7.8	8.1
FeO/SiO_2	0.0	0.0	0.0	0.0	0.0	0.0	0.0	0.1	0.1	0.0	0.0	0.0	0.0	0.0	0.0
Al_2O_3/SiO_2	0.1	0.2	0.1	0.2	0.1	0.2	0.1	0.2	0.2	0.1	0.1	0.2	0.1	0.1	0.1
FeO/K_2O	0.6	0.9	0.5	0.7	1.1	1.1	0.8	1.3	2.5	1.1	1.2	0.3	1.1	1.0	1.0
Co/Th	0.4	0.4		0.6	0.9		0.5			0.6	0.4	0.5		0.7	
Sc/Th	0.3	0.3		0.6	0.7		0.5			0.5	0.5	0.4		0.6	
Th/Sc	4.0	3.0		1.8	1.4		2.1			2.2	1.8	2.6		1.7	
Mineralogy															
Quartz	63.5	64.2	65.2	69.1	66.0	64.7	64.1	50.6	69.5	69.3	66.6	69.0	64.9	67.0	73.4
Feldspar	29.8	27.9	28.3	22.6	24.2	13.4	13.8	27.8	9.6	6.7	16.9	25.6	19.5	15.0	9.5
Mica	5.7	6.4	4.9	7.2	8.1	21.2	21.7	18.6	16.2	3.8	13.1	4.9	9.8	12.7	13.5
Chlorite	1.1	1.4	1.5	1.2	1.7	0.6	0.4	1.6	2.3	2.7	1.7	0.4	1.6	1.3	1.7
Calcite/Dolomite	0.0	0.0	0.0	0.0	0.0	0.0	0.0	0.0	0.0	0.0	0.7	0.0	2.3	3.7	1.0
Amphibole	0.0	0.0	0.0	0.0	0.0	0.0	0.0	1.5	2.4	0.7	1.0	0.0	1.9	0.3	0.9

been grouped as (i) BG (from Bhagirathi River) (ii) AG (Upper reaches of Alaknanda River) (iii) MG (upper reaches of Mandakini River) (iv) AMG (Lower reaches of Mandakini and Alaknanda River) and (iv) GR (the mainstream Ganga River after the confluence of all major tributaries) (Table 1). Three to four kilograms of each sediment sample was collected and air dried and sieved to remove particles above 2 mm size. After homogenization one hundred grams of each sample was taken and was ground to −200 mesh (<75 μm) size in an agate mortar and pestle for geochemical and XRD mineralogical study. The size fractions above 63 μm were determined by dry sieving. For samples having sufficient <63 μm fractions, grain size was measured following the standard pipetting method (Gale and Hoare, 1991) for the silt and clay fraction after treating 50 g of the sample with cold 1 M HCl and H_2O_2 to remove carbonates and organics, and deflocculating the sample by adding sodium hexametaphosphate, and separating the sand by wet sieving. Mineral identification was performed using a Phillips XRD (PW1140). Heavy minerals were separated using bromoform and identified under a binocular microscope. Homogenized powders of sediment samples were digested following the open Teflon beaker acid digestion procedure using a combination of HF, HNO_3, and $HClO_4$ for analysis of major and trace elements. The samples for REE analysis were digested by NaOH and Na_2O_2 fusion method in nickel crucible. REE separation and pre-concentration were done using HNO_3 and HCl cation exchange resin (Bio-Rad AG50-X8 100-200 mesh size, H form) column chemistry (for details see Singh and Rajamani, 2001). All the elements were analyzed using a JY ICP-AES (ULTIMA 2). SiO_2 was determined by a Systronics spectrophotometer following method of Shapiro and Brannock (1962). The precision and accuracy of analysis for major and trace elements including REE by ICP-AES were monitored using USGS rock standards (BHVO-1, STM and RGM-1) as well as in-house rock standards. Data for international reference standards analyzed along with the samples (USGS standard BHVO-1 for major and trace elements, RGM-1 for REE analyzed by ICP-AES and CCRMP Canada standard So-1 (Govindraju, 1994) for Th, Sc, Co, U and Zr analyzed by WD-XRF) are reported in Appendix Table 1A. Both precision and accuracy for major elements are better than 2%, and for trace elements and REE, precision and accuracy are better than 2% and 5% respectively. For low REE samples (<5× chondrite) the precision was 5–10% for Ce and Nd. Blank levels were <0.01 wt.% for most of major elements and below 0.001 for MnO_2 and TiO_2. Blank levels for Ni and Cr is <1.5 ppm, and <0.5 ppm for Ba, Sr and Y. For La, Ce, Nd and Sm it is ≤0.03 ppm, and for Eu, Gd, Dy, Yb and Lu it is ≤0.007 ppm. Concentrations of Zr, Th, Sc, Co, and U on representative samples were analyzed by the XRF method (Siemens SRS3000) at Wadia Institute of Himalayan Geology, Dehradun. The precision and accuracy of the preparation and instrumental performance were checked using international standards (USGS standards SO-1, GXR-2, GXR-6, SCO-1, SGR-1, SDO-1; IGGE China standards GSS-1,GSS-4, GSD-9, GSD-10, GSR-6; CCRMP Canada standard So-1(Govindraju, 1994)) in similar way as outlined in Saini et al. (2002). The precision on repeat measurement for Th, Sc, Co, U and Zr is <3%. The accuracy of measurement is better than 12 % for Th, Sc and Co, and 3% for Zr. For U observed accuracy is 16% (Appendix Table 1A). Calculation of Chemical Index of Alteration (CIA) (Nesbitt and Young, 1984) using molar proportion of Al_2O_3, CaO, Na_2O and K_2O was done on carbonate free basis (see Singh and Rajamani, 2001).

4. Results

4.1. Texture and mineralogy

The mean grain size of the bed load sediments of the Ganga River and its tributaries (Fig. 1) range between 1 Φ and 3.0 Φ (Table 1). The dominant minerals present in the sediments include quartz, plagioclase, K-feldspar, muscovite, biotite and chlorite (Table 1). Some samples contain calcite ranging between 0.7 and 3%. The minor mineral phases present according to the order of their abundance are kyanite/sillimanite, tourmaline and hornblende. Garnet, monazite, zircon and apatite are present in traces. Although mineral proportions show some variations between the samples, the general mineralogy of sediments does not show any variation. Tourmaline is present as euhedral crystals or as elongated shape.

4.2. Geochemistry

The major element and trace elements data, and the REE data of the sediments are given in Tables 1 and 2 respectively.

4.2.1. Major and trace elements

The sediments collected systematically from various locations from river bed of the Ganga River and its three major tributaries, namely Bhagirathi, Mandakini and Alaknanda Rivers, show limited range in composition up to the lowermost location at Haridwar. The observed minor compositional variation, particularly in the abundance of Al_2O_3, TiO_2, FeO, MgO, MnO, Cr and Co, is due to variations in the concentration of silica that ranges between 70% and 80%. This is also reflected in strong to moderate negative correlation between silica and these elements: correlation coefficients are −0.72 for SiO_2–Al_2O_3, −0.78 for SiO_2–TiO_2, −0.74 for SiO_2–FeO, −0.48 for SiO_2–MgO, −0.43 for SiO_2–MnO, −0.52 for SiO_2–Cr, −0.48 for SiO_2–Co and −0.63 for SiO_2–Y. On the contrary, CaO, Na_2O, K_2O, P_2O_5, Ba, Sr, Ni, Sc, Th, U and Zr show no significant correlation with silica.

Table 2
Rare earth element (ppm) composition of the sediments collected from various locations from the Ganga River and its tributaries in the Himalayan catchment region (for locations refer to map).

	Bhagirathi River					Mandakini River				Alaknanda River			The Ganga River		
	(BG Group)					(MG Group)		AMG Group				AG group	(GR Group)		
Sample No.	B1	B2	B3	B4	B5	M1	M2	M3	M4	A2	A3	A1	G1	G2	G3
La	36.3	37.6	20.3	28.0	19.2	57.5	45.2	40.6	44.6	29.3	47.8	26.6	35.3	34.0	26.3
Ce	75.7	80.8	42.0	60.2	40.2	115.5	94.1	81.5	93.1	56.9	100.4	57.7	74.0	70.2	52.2
Nd	34.2	34.3	18.5	26.8	16.8	50.6	40.2	39.5	44.2	23.5	41.8	25.8	31.1	29.5	22.5
Sm	8.4	7.8	4.2	5.9	3.5	11.5	8.4	8.1	8.9	4.5	8.4	5.7	6.4	6.0	4.6
Eu	0.8	0.9	0.6	0.7	0.6	1.5	1.1	0.9	1.0	0.6	1.1	0.6	0.8	0.9	0.7
Gd	7.4	7.4	3.8	5.7	3.2	9.2	7.0	6.8	7.6	3.7	7.2	4.7	5.7	5.0	4.2
Dy	7.2	7.4	3.8	5.5	2.9	7.0	5.1	5.8	6.5	3.3	6.1	5.4	4.9	4.5	3.9
Yb	4.1	4.4	2.4	3.2	1.9	3.3	2.1	2.9	3.3	2.1	3.4	3.1	2.9	2.5	2.3
Lu	0.6	0.6	0.4	0.5	0.3	0.5	0.3	0.4	0.5	0.3	0.5	0.5	0.4	0.4	0.3
(La/Yb)n	6.0	5.9	5.7	6.0	7.0	12.0	14.3	9.5	9.1	9.6	9.4	5.7	8.2	9.1	7.8
(La/Sm)n	2.7	3.0	3.0	3.0	3.4	3.1	3.4	3.1	3.1	4.0	3.5	2.9	3.5	3.5	3.6
(Gd/Yb)n	1.5	1.4	1.3	1.4	1.4	2.3	2.6	1.9	1.9	1.4	1.7	1.2	1.6	1.6	1.5
Eu*/Eu	0.3	0.4	0.4	0.4	0.5	0.4	0.4	0.4	0.4	0.5	0.4	0.3	0.4	0.5	0.5

Table 3
Correlation coefficient among textural and chemical parameters for the entire group of sediments from the mainstream Ganga River and its tributaries in the Himalayan catchment region.

	SiO_2	Al_2O_3	TiO_2	FeO	MgO	MnO	CaO	Na_2O	K_2O	P_2O_5	CIA	Mz	Ba	Sr	Cr	Ni	Sc	Co	Th	U	Zr	La	Ce	Nd	Sm	Eu	Gd	Dy	Yb	Lu
SiO_2	1																													
Al_2O_3	−0.75	1.00																												
TiO_2	−0.70	0.20	1.00																											
FeO	−0.75	0.28	0.92	1.00																										
MgO	−0.55	−0.06	0.81	0.68	1.00																									
MnO	−0.39	−0.05	0.66	0.83	0.38	1.00																								
CaO	−0.33	−0.33	0.63	0.53	0.85	0.47	1.00																							
Na_2O	−0.17	0.63	−0.53	−0.40	−0.57	−0.52	−0.66	1.00																						
K_2O	−0.35	0.71	−0.29	−0.27	−0.31	−0.49	−0.50	0.83	1.00																					
P_2O_5	−0.31	0.41	0.12	0.08	−0.17	0.06	−0.05	0.25	0.15	1.00																				
CIA	−0.18	0.52	−0.09	0.01	−0.28	−0.08	−0.40	0.31	0.19	0.03	1.00																			
Mz	−0.16	0.22	−0.19	−0.29	0.22	−0.61	0.10	0.29	0.43	−0.16	0.11	1.00																		
Ba	−0.37	0.29	0.18	0.27	0.25	0.14	0.15	0.00	0.10	0.25	0.28	0.21	1.00																	
Sr	−0.37	−0.01	0.28	0.36	0.45	0.36	0.61	−0.20	−0.19	0.36	−0.10	0.14	0.75	1.00																
Cr	−0.54	0.29	0.31	0.27	0.51	0.00	0.34	0.13	0.34	−0.13	−0.30	0.30	0.05	0.21	1.00															
Ni	−0.40	0.42	0.23	0.16	0.14	−0.10	−0.10	0.31	0.40	0.15	0.16	0.00	0.15	0.05	0.52	1.00														
Sc	−0.41	−0.26	0.51	0.58	0.68	0.36	0.68	−0.48	−0.25	−0.39	0.19	0.46	0.65	0.57	0.01	−0.19	1.00													
Co	−0.39	−0.14	0.62	0.81	0.66	0.17	0.25	−0.35	−0.14	−0.61	−0.05	0.36	0.59	0.14	0.02	−0.08	0.55	1.00												
Th	−0.02	0.14	−0.14	−0.21	−0.37	−0.01	−0.02	0.20	−0.06	0.75	0.34	−0.40	0.15	0.27	−0.38	0.25	0.09	−0.41	1.00											
U	−0.08	0.80	−0.56	−0.65	−0.78	−0.60	−0.77	0.58	0.71	0.44	0.35	−0.07	0.05	−0.36	−0.29	0.17	−0.45	−0.35	0.24	1.00										
Zr	−0.31	−0.01	0.07	0.09	0.05	0.16	0.36	0.03	−0.14	0.43	0.33	−0.06	0.42	0.64	−0.01	0.34	0.45	−0.20	0.85	−0.13	1.00									
La	−0.53	0.29	0.46	0.46	0.29	0.40	0.41	−0.10	−0.07	0.75	0.12	−0.09	0.63	0.75	−0.07	0.13	0.47	−0.04	0.77	−0.04	0.85	1.00								
Ce	−0.52	0.30	0.42	0.44	0.25	0.39	0.38	−0.06	−0.05	0.73	0.17	−0.09	0.62	0.74	−0.11	0.13	0.47	−0.06	0.79	−0.01	0.88	1.00	1.00							
Nd	−0.62	0.41	0.48	0.52	0.25	0.45	0.36	−0.01	−0.01	0.75	0.21	−0.11	0.59	0.70	−0.04	0.16	0.41	−0.14	0.84	0.07	0.89	0.98	0.99	1.00						
Sm	−0.55	0.46	0.34	0.39	0.10	0.33	0.21	0.13	0.06	0.81	0.29	−0.11	0.59	0.66	−0.09	0.18	0.23	−0.28	0.93	0.18	0.90	0.96	0.96	0.98	1.00					
Eu	−0.54	0.34	0.41	0.43	0.32	0.29	0.36	−0.03	−0.01	0.68	0.17	0.04	0.78	0.81	−0.01	0.15	0.59	0.17	0.68	−0.12	0.85	0.96	0.95	0.93	0.93	1.00				
Gd	−0.51	0.46	0.31	0.38	0.06	0.31	0.16	0.14	0.03	0.76	0.41	−0.14	0.57	0.61	−0.14	0.23	0.22	−0.27	0.95	0.21	0.92	0.92	0.93	0.95	0.98	0.89	1.00			
Dy	−0.37	0.48	0.10	0.19	−0.21	0.20	−0.08	0.31	0.11	0.70	0.56	−0.20	0.32	0.37	−0.20	0.33	−0.07	−0.55	0.89	0.34	0.80	0.71	0.75	0.78	0.85	0.65	0.91	1.00		
Yb	−0.11	0.29	−0.06	0.00	−0.33	0.09	−0.18	0.28	0.01	0.49	0.59	−0.29	0.04	0.11	−0.25	0.37	−0.17	−0.64	0.77	0.23	0.70	0.43	0.48	0.50	0.59	0.35	0.69	0.91	1.00	
Lu	−0.11	0.33	−0.11	−0.03	−0.37	0.08	−0.22	0.34	0.06	0.54	0.58	−0.28	0.08	0.14	−0.27	0.33	−0.23	−0.69	0.76	0.30	0.65	0.45	0.50	0.52	0.63	0.38	0.71	0.92	0.99	1.00

The poor correlation of Al_2O_3 with all elements, except with Na_2O, K_2O and U, (Table 3) suggests negligible chemical weathering and sorting. Strong correlation among Na, K, Al and U indicates feldspars (potassic and sodic) and muscovite as the dominant host for these elements in the sediments. Strong correlation of Ba to Sr, indicates their control by similar mineral phases, probably the feldspars, mica and may be calcite. Correlation coefficients of 0.94 between Fe and Ti, 0.68 for Fe and Mg, 0.84 for Fe and Mn, and 0.82 for Ti and Mg, suggests them to be housed in similar mineral phases, probably biotite, muscovite and garnet. Strong positive correlation of Th to P_2O_5 (0.76), Zr (0.85) and Y (0.55), indicates their presence in monazite and zircon. Similar strong correlation between Zr and Y (0.85) indicates control by zircon.

Careful examination of the sediments revealed that the samples from lower reaches of Bhagirathi River (sample B5), Alaknanda River (sample A2 and A3), Mandakini River (sample M3 and M4) and from the Ganga River (GR) have relatively higher concentration of FeO, MgO and CaO (Table 1). This indicates that there was only minor addition of amphibole and/or calcite to the sediments during the course of the rivers through the lower part of HHCS and/or Lesser Himalayas.

4.2.2. Comparison with average sandstone and UCC

The studied sediments are notable for their low Al_2O_3/Na_2O (3.2–5.7) and K_2O/Na_2O (0.7–1.4) ratios (Table 1) compared to most other sandstones indicating chemical immaturity of these sediments, and their derivation from relatively unweathered source (Taylor and McLennan, 1985; McLennan et al., 1993). This is also indicated by concentrations of all elements a few order higher than the average sandstone (Condie, 1993) (Fig. 2). In comparison with sandstone Na_2O, K_2O, P_2O_5, Ba, Sr, Sc, Co, Th and U show manifold higher concentration.

The upper continental crust (UCC) (Taylor and McLennan, 1985) normalized pattern for major and trace elements (Fig. 3) indicates that the sediments are depleted in Al_2O_3, TiO_2, FeO, MgO, CaO, Na_2O, K_2O and Ba, and more so in Sr, Cr, Ni, Sc, and Co. Minor depletion in Al_2O_3, Na_2O, K_2O, CaO is clearly due to the dilution effect of silica. Depletion in TiO_2, FeO, MgO, Sr, Cr, Ni, Sc and Co, apart from the dilution effect of silica, could also be due to fractionation by fluvial processes leading to preferential removal of fine grained mica group of minerals as suspended load in comparison to feldspars. This is further corroborated by the observed higher mica percentage in the suspended load (Chakrapani, 2005) compared to the bed load examined in this study.

In contrast to the above set of elements, the sediments show enrichment of SiO_2, P_2O_5, Th, U, Zr and Y compared to UCC. Higher abundance of U once again indicates lower chemical weathering.

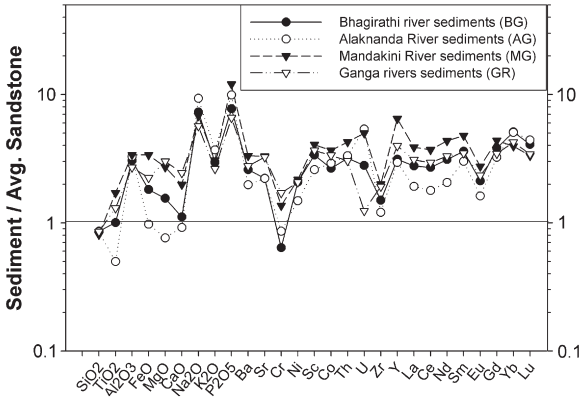

Fig. 2. Average major, trace and rare earth element concentration of the sediment samples from various tributaries and the Ganga River after their confluence in the Himalayan region normalized to composition of average sandstone (Condie, 1993).

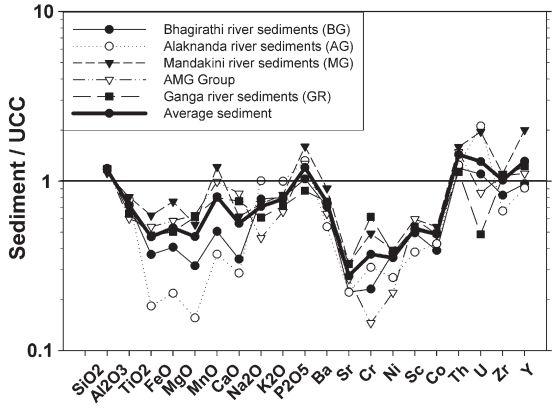

Fig. 3. Average major and trace element concentration of the sediment samples from various tributaries and the Ganga River in the Himalayan region normalized to the composition of average UCC (Taylor and McLennan, 1985).

Enrichment of P_2O_5, Th, Zr and Y could be either due to higher abundance of these elements in the source or concentration of heavy minerals such as monazite, apatite and zircon in the sediments.

4.2.3. Rare earth elements

The REE concentrations of bulk sediments from the three major tributaries of the Ganga River namely Bhagirathi (BG), Mandakini (MG) and Alaknanda (AG) Rivers, Alaknanda and Mandakini in lower reaches and after their confluence at Rudraprayag (AMG), and of the Ganga River (GR) after the confluence of the above tributaries are listed in Table 2. The REE concentrations in the suspended sediments of Bhagirathi, Alaknanda and the Ganga Rivers (Chakrapani, 2005) are also listed in Table 4.

The total REE of the sediments ranges between 81 and 262 with the average value of 155. Among the several compositional variables of the sediments, Th, Zr and P_2O_5 show strong positive correlation with all the REEs (Table 3), which indicates control of monazite, zircon and apatite on the REE distribution. Interestingly LREE has a good correlation with Ba and Sr that indicates control of muscovite and feldspar on it.

The sediments can be differentiated into three groups based upon their distinct REE patterns. The first group includes sediments from BG and AG that exhibit similar less fractionated parallel to sub parallel chondrite normalized REE patterns (Fig. 4a and c). The La_N/Yb_N value for BG ranges from 5.7 to 7 and is 5.3 for AG (Table 2). In contrast, the second group, which includes sediments from MG, displays more fractionated chondrite normalized REE patterns (Fig. 4b) with La_N/Yb_N value ranging from 12.0 to 14.3. The third group, which includes

Table 4
Rare earth element (ppm) composition of the suspended sediments collected from various tributaries and the mainstream Ganga River around Devprayag (Chakrapani, 2005).

	Bhagirathi at Devprayag	Alaknanda at Devprayag	The Ganga at Devprayag
La	37.1	29.9	34.5
Ce	79.5	60.4	70.4
Pr	9.02	6.87	8.09
Nd	32.9	25	30.1
Sm	7	4.85	6.1
Eu	1.01	0.953	0.99
Gd	6.74	4.54	5.3
Tb	1.11	0.69	0.822
Dy	6.55	3.77	5
Ho	1.38	0.733	0.95
Er	3.89	2.01	2.71
Tm	0.621	0.315	0.421
Yb	4.18	2.08	2.74
Lu	0.582	0.303	0.411

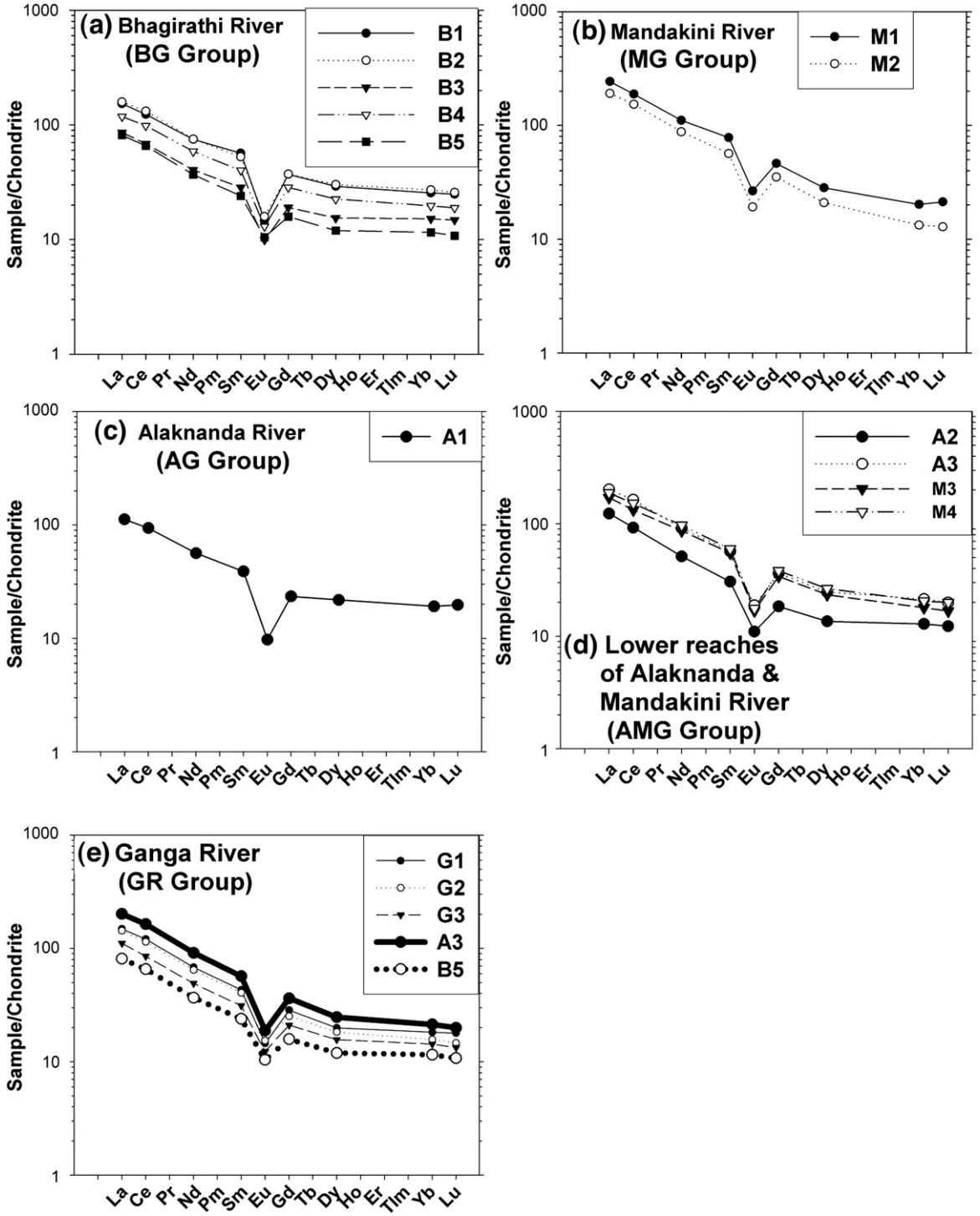

Fig. 4. Chondrite normalized REE pattern of sediment collected from (a) Bhagirathi river (BG group) (b) Mandakini River (MG group) (c) Alaknanda River (AG group) (d) Alaknanda and Mandakini Rivers in lower reaches (AMG group) and (e) the Ganga river (GR group) in the Himalayan catchment region after the confluence of all the above tributaries. Note that the samples from Bhagirathi and Alaknanda rivers are less fractionated compared to Mandakini River which shows greater fractionation. Samples from AMG group and the Ganga River show intermediate fractionation. Also note the deep negative Eu anomaly in all the samples indicating fractionated source rocks. Chondrite values from McDonough and Sun (1995).

sediments from AMG and GR, exhibits similar parallel to sub parallel REE patterns (Fig. 4d) with La_N/Yb_N ratios ranging from 7.8 to 9.5 (Table 2). Thus it is seen that the La_N/Yb_N ratios of third group (AMG and GR) of sediments, are intermediate between that of first group (AG and BG) and the second group (MG) sediments collected from the HHCS traverse. This indicates, that the REE patterns of AMG and GR groups of sediments could be a result of mixing of sediments from the aforesaid two end member groups (first and second group) draining the HHCS. The GR group of sediments, sampled at various locations after Devprayag up to Haridwar, exhibits no change and maintains similarly fractionated parallel REE patterns in this segment. Therefore, it can be inferred that the resultant REE patterns of the sediments in the lower reaches of the tributaries and the Ganga River, are the product of mixing of sediments supplied by the tributaries draining the HHCS lithologies. This would imply that there was no major lateral addition of sediments from the LH region in this part, which otherwise

would have brought some variations in the chemistry; secondly the sediments have been mineralogically well homogenized much before reaching Haridwar, after which the Ganga River enters into the Plains region.

The La_N/Sm_N values for the sediments from all the above rivers vary within narrow range from 2.7 to 4.0 and in general exhibit higher LREE fractionation. In contrast, the Gd_N/Yb_N ratios exhibit larger variations between the above groups of sediments. The Gd_N/Yb_N ratio ranges between 1.2 and 1.6 for BG and AG, and between 2.3 and 2.6 for MG, and between 1.5 and 1.7 for AMG and GR groups of sediments. Thus the observed variation in La_N/Yb_N ratios is largely due to the variation in Gd_N/Yb_N ratios (1.2 to 2.6). This is corroborated by strong positive correlation of La_N/Yb_N with Gd_N/Yb_N (0.9), in comparison to moderate correlation between La_N/Yb_N and La_N/Sm_N (0.5). Amongst all the variables, Gd_N/Yb_N shows good correlation with P_2O_5 (0.57), Ba (0.69) and Sr (0.6), and poor correlation with Zr (0.32) and Th (0.33). This would imply that variation in Gd_N/Yb_N is mainly because of variation in minerals containing P_2O_5, Ba and Sr, which in the present case are monazite, apatite, muscovite and biotite. Poor correlation among Gd_N/Yb_N and Th is probably because Th, in addition to monazite, also has other sources, particularly zircon. The sediments from Mandakini River (MG) have highest P_2O_5 concentration and correspondingly highest Gd_N/Yb_N ratios. Thus the observed variations in the REE patterns seemingly reflect variation in the REE hosting minerals. Such mineralogical variations could be because of process related mineral sorting or because of the differences inherited from their source.

Sediments from all the rivers show consistently marked negative Eu anomalies, with $(Eu/Eu^*)_N$ ratios ranging between 0.27 and 0.53, with an average value of 0.42. In the $(Eu/Eu^*)_N$ vs. Gd_N/Yb_N diagram (Fig. 5) all the sediments, except the two from Mandakini River (MG), plot in the field with Gd_N/Yb_N ratio <2 and $(Eu/Eu^*)_N$ <0.85. The lower values of Eu anomalies, indicate that the sediments have been derived from a highly differentiated source (Taylor and McLennan, 1985). It should also be noted that the channel sand of these rivers have not undergone much mineralogical sorting, as otherwise feldspars are expected to be preferentially concentrated in the channel sand along with quartz, which could result in either reduced or positive Eu anomaly (Bhatia, 1985; Singh and Rajamani, 2001). This would imply that the sediments are simply the ground up rocks, and the mineral separation and sorting has been inefficient. In such case, the bed load sediments should have chemistry similar to that of the suspended load. To check this premise, I have compared the UCC normalized REE patterns of the bed load sediments collected from different parts of the rivers in this study, with that of the suspended load reported from the same sectors (Chakrapani, 2005).

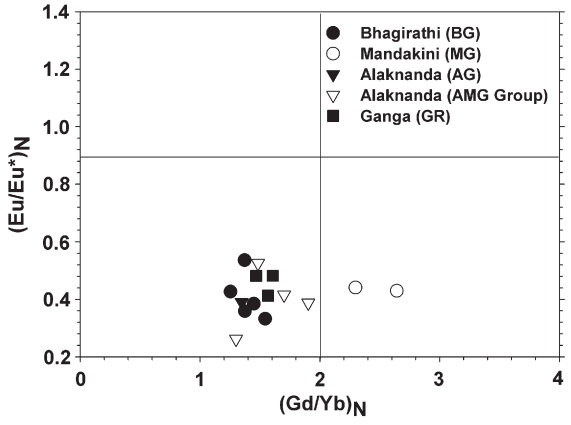

Fig. 5. Plot of Eu/Eu* vs. (Gd/Yb)n for sediments from various tributaries. All the sediments are significantly depleted in Eu (lower Eu/Eu*) indicating their source rocks to have been produced by massive intracrustal melting.

It is interesting to note the similarity in UCC normalized REE patterns, between the suspended sediment from Bhagirathi River and its bed load (BG) (Fig. 6a); suspended sediment from Alaknanda River before Devprayag and its bed sediment (AMG) (Fig. 6d); and suspended sediment from the Ganga at Rishikesh after Devprayag and bed sediments from the Ganga River (GR) after the confluence of all these tributaries (Fig. 6e). This would suggest that the significant negative Eu anomalies, present in all the sediments, are not due to the influence of the fluvial process of mineral sorting but represents the characteristic of their source.

The UCC normalized REE patterns of all the sediments from the Bhagirathi River (BG) are similar, although they vary in their abundance (Fig. 6a). All the samples from this river show significant enrichment of MREE and HREE, and a significant depletion of Eu in comparison to the UCC. The REE patterns of the sediments do not change even after the river has entered into the Lesser Himalayan zone from the Higher Himalaya. Similar MREE and HREE enrichment, and depletion of Eu in comparison to the UCC is also observed in AG sediment from Alaknanda River (Fig 6c). By implication, the BG and AG sediments have been derived from the similar sources. The UCC normalized REE patterns of MG sediments, from Mandakini River, exhibit similar LREE patterns and enrichment of MREE with marked negative Eu anomaly. But contrary to BG and AG, MG sediments show highly fractionated HREE pattern (Fig. 6b) possibly indicating different source lithologies. However, this could also be due to the enrichment of monazite/apatite in these sediments, as indicated by their higher concentrations of P_2O_5.

Thus, to a first approximation it can be inferred that (i) the REE patterns of the sediments from the primary tributaries are similar to their sources in the HHCS and the changes observed after their confluence, is a result of their mixing. The latter may be inferred from the attainment of intermediate REE patterns of the joining tributaries; (ii) there was not much addition of sediments from en route lithologies of catchment i.e. Lesser Himalayas and the Siwaliks Himalaya; (iii) not much mineralogical sorting had taken place as indicated by the similarity of REE patterns of suspended and bed load sediments and (iv) the sediments have been derived from highly differentiated source, as indicated by marked negative Eu anomalies of all the sediments in comparison to the UCC.

5. Discussion

5.1. Sediment maturity and weathering

The hydrological differentiation processes that operate on river sediments combined with source rock composition and chemical weathering tend to produce sediment suites with different chemical composition (Nesbitt and Young, 1989; Frallick and Kronberg, 1997). With increased maturity of the sediments, there is an increase in quartz at the expense of feldspar, mafic minerals and lithic fragments in the bed sediments. This results in an increase of SiO_2 and decrease of major elements like Na, K, Ca, Al, Fe, Mg and some other trace elements in the bed load sediments. This affects the ratios of some elements, such as SiO_2/Al_2O_3, Na_2O/K_2O, FeO/K_2O and FeO/SiO_2, which in turn serve as good indicators of sediment maturity (Pettijohn et al., 1972; Herron, 1988). With increased sediment maturity, SiO_2/Al_2O_3 ratios are increased, while FeO/SiO_2 and Al_2O_3/SiO_2 ratios are decreased. The ratios such as Na_2O/K_2O and FeO/K_2O, indicate the differential stability of feldspar and Fe and K-bearing minerals. The entire groups of sediments studied from the mainstream Ganga River and its tributaries in the mountainous region of Himalaya, plot in the litharenite field of log Na_2O/K_2O vs. SiO_2/Al_2O_3 diagram (Fig. 7a) of Pettijohn et al. (1972). In log (SiO_2/Al_2O_3) vs. log (FeO/K_2O) scheme of Herron (1988), the sediments occupy the field of litharenite and arkose (Fig. 7b). AMG and GR group of sediments show slight increase of SiO_2 and an apparent loss of Na_2O, as seen in their higher SiO_2/Al_2O_3

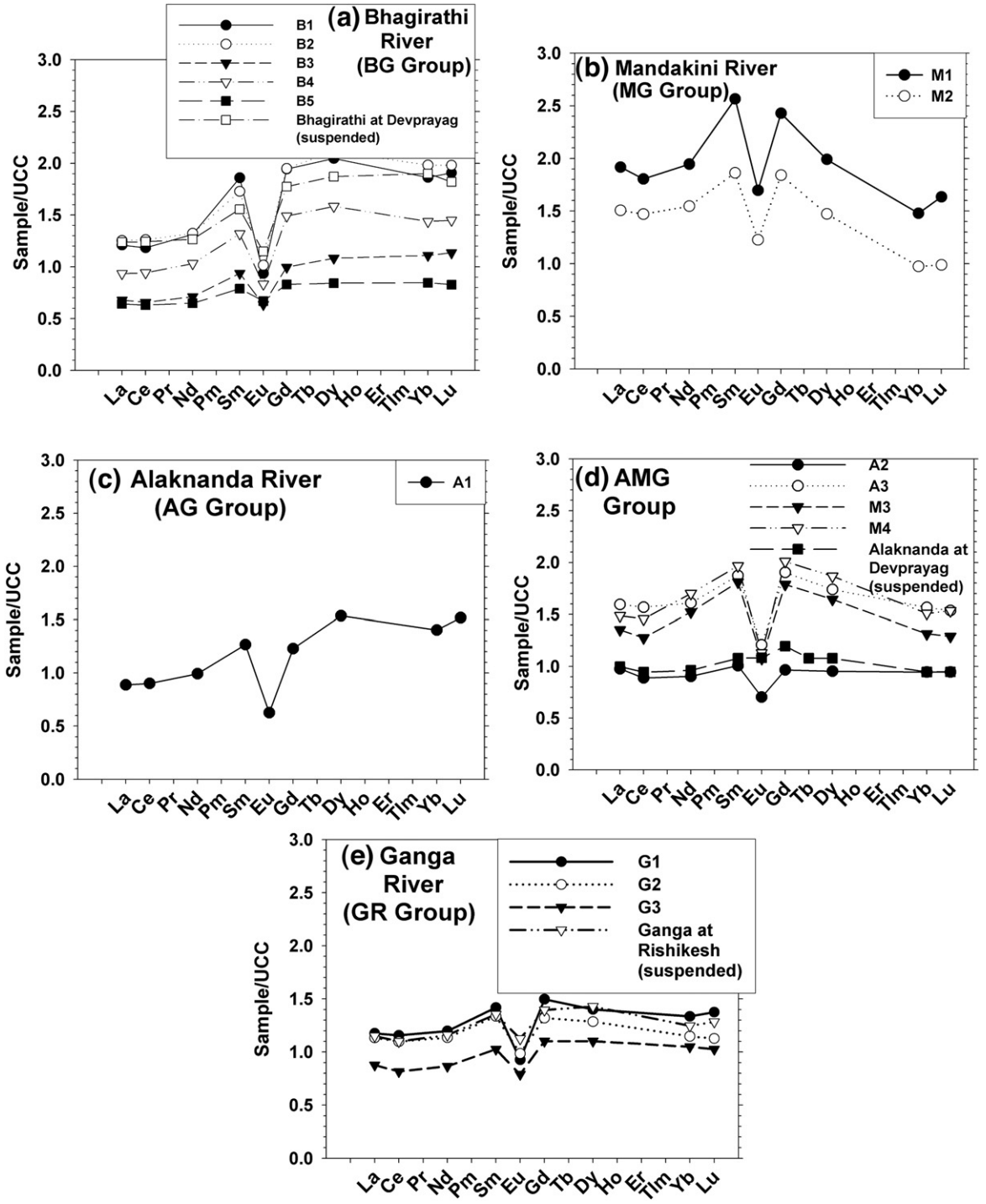

Fig. 6. UCC normalized REE pattern of sediment collected from (a) Bhagirathi river (BG group) (b) Mandakini River (MG group) (c) Alaknanda river (AG group) (d) Alaknanda and Mandakini Rivers in lower reaches (AMG group) and (e) the Ganga river (GR group) along with the plot of suspended sediment (Chakrapani, 2005). Note the sediments from BG and AG group show enrichment in MREE and HREE compared to UCC, whereas Mandakini River sediments show only MREE enrichment; also note the similarity of UCC normalized REE pattern and abundance between suspended and bed load.

and lower Na_2O/K_2O ratios, although the change is not very significant. The slight lowering of Na_2O/K_2O ratio is probably due to en route weathering of the sediments during their traverse through changing topography and climate in the Lesser Himalayan region. Observed higher variation in FeO/K_2O ratios, seems unrelated to the process but source controlled. This is evident from the fact that the AMG and GR groups of sediments from the lower reaches, have compositions intermediate between that of the two end member tributaries i.e. BG and AG (first group) and MG (second group). Similar phenomenon is also observed in case of REEs. This implies that the two end member sources have similar feldspar component as evident by their similar Na_2O/K_2O ratios, but varies in Fe-bearing minerals. The aforesaid observations made on the basis of the geochemistry, suggest that the sediments are immature and have suffered little mineralogical sorting, which has, to some extent, affected only the distribution of mica group of minerals between the suspended and bed load. This is evident by moderate negative correlation of Fe, Mg and Ti to SiO_2 in the sediments. Feldspars have not at all been affected

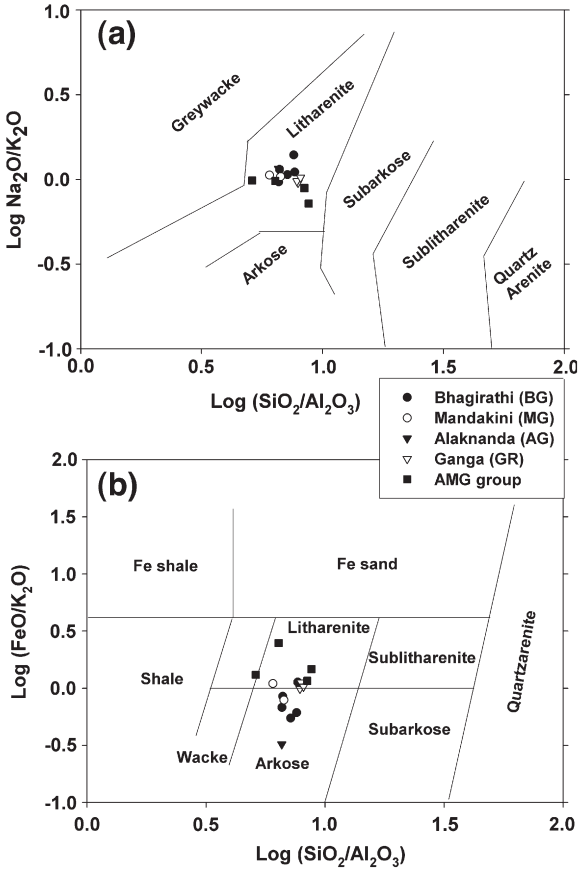

Fig. 7. (a) Plot of all the sediments in Log Na_2O/K_2O vs. Log $SiO_2/Al2O_3$ diagram (Pettijohn et al., 1972) (b) Plot of all the sediments in Log FeO/K_2O vs. Log $SiO_2/Al2O_3$ diagram (Herron, 1988). Note that all the sediments plot in Litharenite field in (a) and Litharenite and Arkose fields in (b) indicating towards immaturity of sediments.

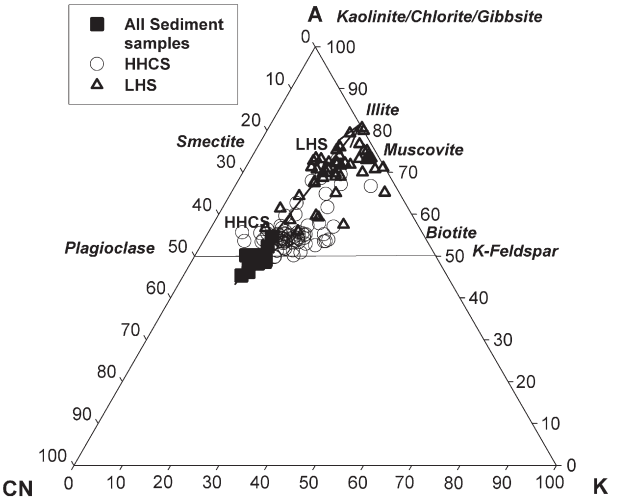

Fig. 8. Plot of all the sediments in the A–CN–K diagram. For comparison are also plotted HHCS and LHS rocks (Harris et al., 1992; Ayres and Harris, 1997; Ahmad et al., 2000; Galy and France-Lanord, 2001; Miller et al., 2001; Rashid, 2005; Richards et al., 2005) from the catchment region. Note that all the samples plot along the feldspar join suggesting unweathered nature of sediments and the overlap of the sediments with the field of HHCS rocks indicates it to have acted as the source rock. Lesser Himalayan rocks (LHS) plot much above the sediments indicating them to have been derived from much weathered precursor.

by sorting as seen by very poor correlation of Na_2O, K_2O, CaO, Ba, and Sr to SiO_2. Even the similarity between the REE patterns of the suspended and the bed load observed earlier, suggests little or no mineral fractionation. The above observations suggest that the sediments have been derived from the source, which has not undergone much chemical weathering and the sediments are just the ground up product of the source rocks.

The weathering history of the source can be examined by the relationship among alkali and alkaline earth major elements (Na_2O, K_2O and CaO), and Al_2O_3 in the silicate phases (Nesbitt and Young, 1984). Accordingly a parameter known as the CIA (the chemical index of alteration), which is $[Al_2O_3/(Al_2O_3 + CaO^* + Na_2O + K_2O)] \times 100$ in molecular proportions, (where CaO* is the amount of CaO incorporated in the silicate fraction of rocks) quantitatively indicates the degree of weathering. The CIA values of the entire groups of sediments range between 47.9 and 54.7 (Table 1), which is similar or even less than the CIA value of the UCC. The range of CIA suggests that the sediments have been derived from the source rocks that have only undergone physical breakdown without any chemical weathering. In the A–CN–K diagram (Fig. 8), the river sediments are plotted along with the potential parent source rocks from different parts of the Himalaya through which the river passes i.e. different lithologies of Higher Himalaya, Lesser Himalaya and the Siwaliks. The sediments plot near to that of UCC and closer to the various lithologies of Higher Himalaya. The rocks of LH along with that of Siwalik group of sediments, are seen to plot as a separate cluster much above the plots for the sediments. The clustering of all the sediments in a narrow field suggests that even Ca and Na have not been mobilized. The sediments in general show a trend moving slightly away from the A–CN line, indicating some loss or removal of K_2O to the suspended load in the form of mica. The little shift downward on the trend line compared to above source rocks, is probably due to minor fractionation by fluvial processes whereby part of the fine grained mica group of minerals, as also seen earlier, have been removed as suspended load in preference to feldspars, leading to slight lowering in the concentration of K_2O and Al_2O_3. This becomes evident on comparing the mineral composition of the suspended load from the Himalayan region (Chakrapani, 2005) with that of the channel sediments in this study. The suspended sediment has higher mica and lower feldspar percentage, compared to the bed load sediments. This is also observed in the Fe/Si vs. Al/Si plot (Fig. 10e), in which the sediments show shift towards the quartz end and away from biotite/muscovite end relative to the probable source rocks. From the foregoing discussion it appears that the sediments have not experienced much chemical weathering, and little shift away from source rocks is due to minor influence of sorting, and the sediments have predominantly been derived from the various lithologies of the HHCS rocks.

The above results corroborate the finding of Quade et al. (1997), who based upon the $^{87}Sr/^{86}Sr$ isotopic ratios of detrital and pedogenic carbonates from Siwalik sediments, inferred that the rise in Sr isotopic ratio in the ocean since the Himalayan uplift was not because of silicate but carbonate weathering. Singh (2009) in his geochemical study of the sediments from the Ganga River in the Plains, has noted that although these sediments after entering into the Gangetic Plains had suffered greater chemical weathering compared to sediments from the catchment region, it has still not proceeded to a significant level. Similarly Jacobson et al. (2002) in their study have concluded that at least ~76% of Sr in the Himalayan stream water is derived from carbonate weathering.

The above observations have important repercussion on the Cenozoic Global cooling theory of Raymo and Ruddiman (1992), who predicted an increased rate of CO_2 drawdown and consequent global cooling as a result of enhanced silicate weathering associated with Himalayan uplift during this time.

Another major change reported during the Cenozoic is the expansion of C_4 vegetation particularly during the Late Miocene. The studies carried out on paleosols from various exposed sections of Siwalik sediments from Pakistan, Nepal and India have reported

abrupt change in the vegetation from dominantly C_3 plants to C_4 grasses around 7 Ma. This shift in vegetation is now established to have occurred world over. Quade et al. (1995) and Cerling et al. (1997) based upon their studies on stable carbon isotope compositions of organic matter and pedogenic carbonates, have suggested this change as a result of reduction in atmospheric CO_2 during this time, which they have attributed to the chemical weathering. Retallack (1991, 2004, 2009) found similar shift in vegetation in his studies carried on paleosols from Indian subcontinent, Kenya and North America, and have also reported change in the mammalian species due to the vegetation change. He has proposed that the spread of C_4 grass was not as a result of reduced level of atmospheric CO_2 and associated global cooling, but the spread of C_4 grasslands was itself the cause of CO_2 drawdown and consequent global cooling. He has suggested that the fall in atmospheric CO_2 level was a result of carbon sequestration and consumption by grassland soils and sediments, which along with higher albedo of grasslands resulted in gradual fall in atmospheric temperature and global cooling culminating into ice age around later part of the Cenozoic (~1.8 Ma). The results of the present study and study carried out by Singh (2009) also indicate lower degree of silicate weathering in consonance with the studies on paleosols by Retallack (1991). In this context the theory of climate change as envisaged to have been induced by changes in the chemical weathering due to Himalayan uplift needs to be re-looked. To resolve the debate on late Cenozoic global cooling, more data set is needed on the chemistry of the sediments from other rivers draining the Gangetic Plain and originating from different parts of the Himalaya.

5.2. Provenance

Some elements, particularly their ratios are useful indicators of the provenance as they are least affected by different processes such as weathering, transport and sorting. In particular the immobile elements, such as Th, Sc, Co, Cr, REEs and their ratios have been found to be useful (Taylor and McLennan, 1985) for provenance studies. These elements have short residence time in water and therefore, are almost quantitatively transferred into the sediments. The ratios and the plots between Co/Th vs. La/Sc, and Co/Th vs. Sc/Th, help us to distinguish between the mafic and the felsic source of the sediments, as they include both compatible and incompatible elements (Taylor and McLennan, 1985; Bhatia and Crook, 1986; McLennan and Taylor, 1991; Bauluz et al., 2000). Thorium and lanthanum are typically more concentrated in granitic rocks, and Cr, Sc and Co are enriched in basic rocks. Thus, Th/Sc, Th/Co, La/Sc ratios for fractionated crust are high and low for basic rocks. Typically for post Archean UCC the ratio of Th/Sc is ~1 and for granitic rocks still higher, and for Archean and basic rocks it is less than 1.

The elements, La, Th and Sc are compared in La–Th–Sc ternary diagram (Fig. 9a). In this diagram the sediments cluster around UCC, and between granite and granodiorite field. Similarly in the plots of elemental ratios, such as Co/Th vs. La/Sc, and Co/Th vs. Sc/Th the sediments plot between UCC and granite (Fig. 9b). The above results indicate that the sediments were derived from the mixing of granitic and granodioritic rocks, and had negligible contribution from the mafic rocks. Marked negative Eu anomalies, with $(Eu/Eu^*)_N$ ratios ranging between 0.27 and 0.53 with average value of 0.42 and Th/Sc values ranging between 1.4 and 4.0 in sediments, also corroborate the above observation that the studied sediments were derived from differently fractionated felsic source rocks. For this reason in the following discussion I have compared the studied sediments only with various felsic lithologies present in the catchment region.

The probable source rocks considered for comparison from the HHCS are, the Mio-Pliocene leucogranites (Ayres and Harris, 1997), Proterozoic to early Paleozoic metasediments (Harris et al., 1992; Richards et al., 2005), Cambro-Ordovician biotite/muscovite granite (Miller et al., 2001), Vaikrita and Munsiari gneiss and schist (Ahmad et al., 2000). From the LHS, gneisses and schist from Ramgarh group, shales and sandstones from Chandpur formation (Ahmad et al., 2000), and pelites from Rautgara and Chakrata formations (Rashid, 2005) are taken into consideration.

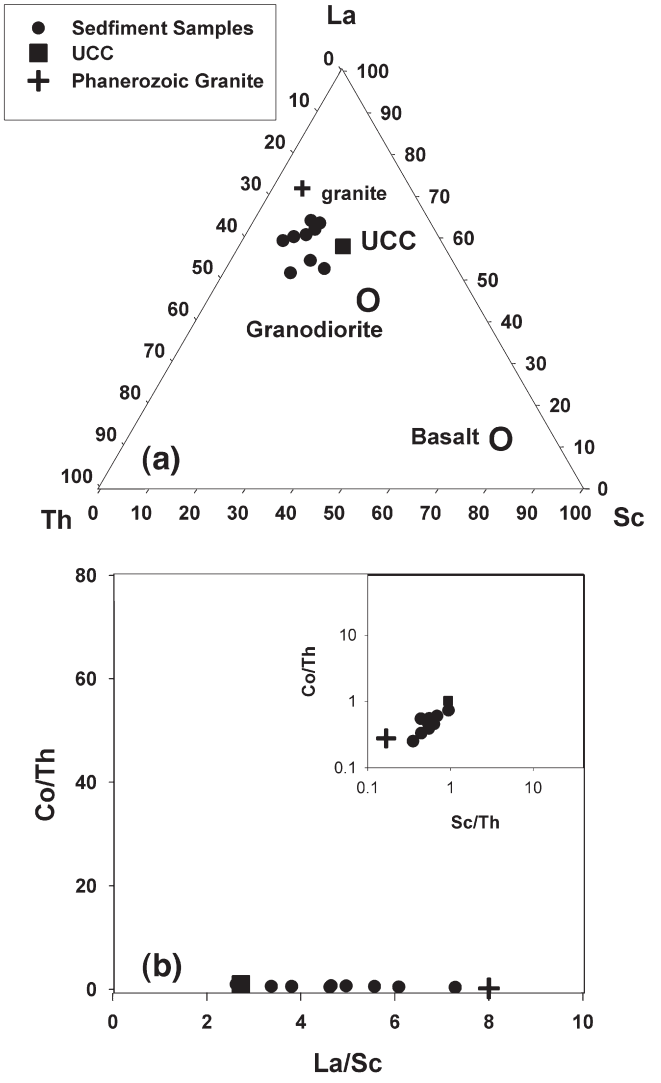

Fig. 9. Plot of selected samples in the (a) La–Th–Sc ternary plot diagram and (b) Co/Th vs. La/Sc and Co/Th vs. Sc/Th binary diagram. Note that all the samples plot in-between the field of average Granite and Granodiorite indicating the source rock to be of granite/granodiorite composition.

5.3. Comparison of major and trace element

Since, in the foregoing sections it had been inferred that the chemical weathering and hydraulic sorting did not significantly affect the chemical composition of the studied sediments, and the sediments represent the mechanically ground up source rocks, it is appropriate in the present case to take into consideration different elements, including the so-called mobile elements for determination of the source.

The major elements (FeO, TiO_2, MgO, Na_2O, K_2O, Al_2O_3 and SiO_2) that are associated with major minerals constituting the studied sediments, are compared with the Himalayan source rocks in various binary diagrams (Fig. 10 a–e). The data for different source lithologies are taken from the various published sources listed above.

Considering first the alkali elements, mostly present in the feldspars, sediments and the probable source lithologies have been plotted in Na_2O vs. K_2O binary diagram (Fig. 10a). All the sediments collected from

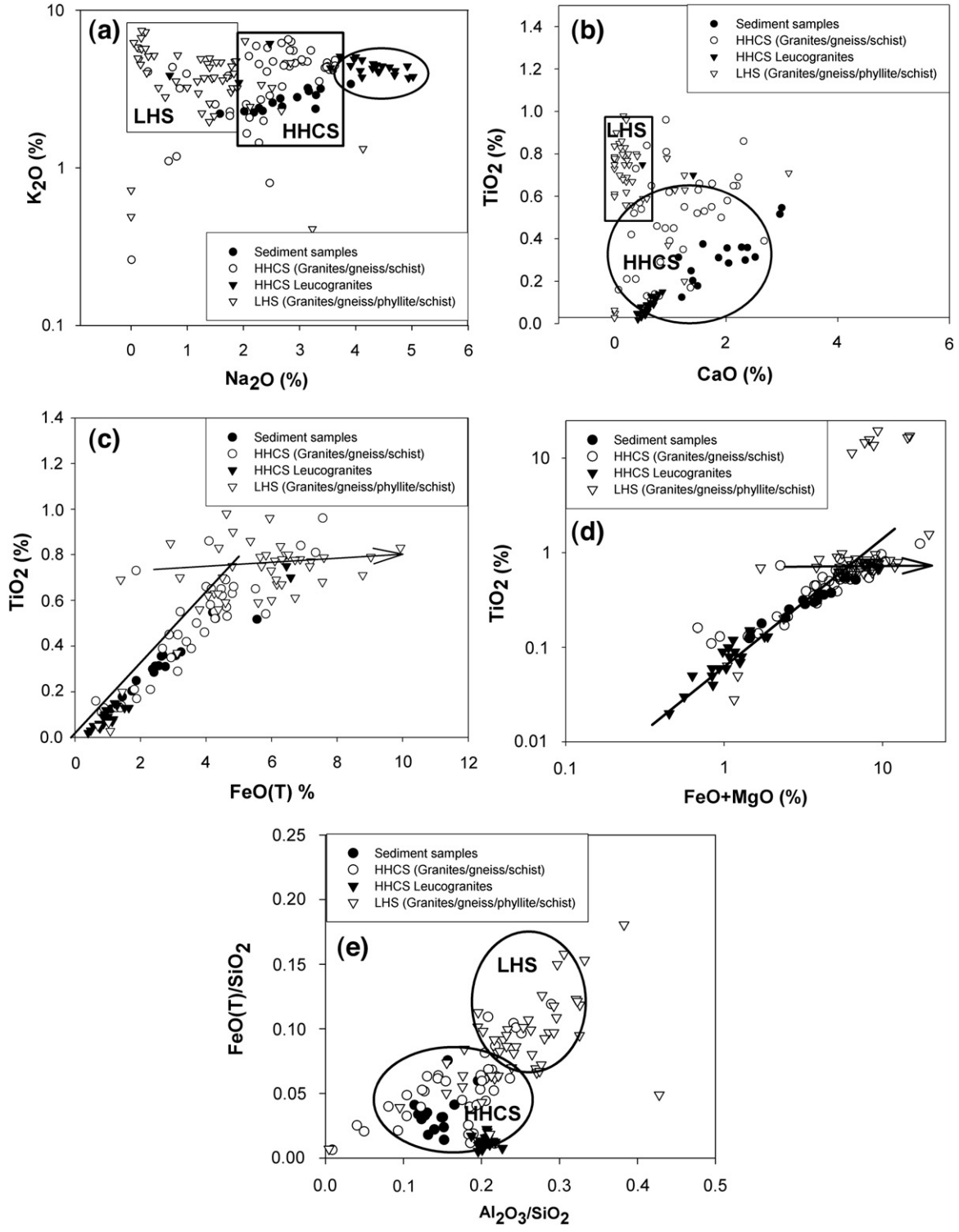

Fig. 10. Plots of sediments in the bivariant diagram between different elements and their ratios. Note that the sediments fall either in the field of HHCS rocks (a,b, and e) or show similar trend (c and d), whereas LHS rocks plot in different field or show different trend line. This clearly suggests HHCS to have acted as the predominant source to the sediments.

the river, when passing through different sections of HHCS and LHS, plot in the field of HHCS. Importantly, the sediments have higher Na_2O than the LH rocks. In general, the sediments are expected to have lower concentration of mobile elements such as Na, Ca, K etc. compared to their sources, as these are first to be mobilized even at the stage of incipient weathering. Higher concentration of Na_2O compared to the LH rocks, implies that there was an insignificant input from the LH rocks into the sediment load of the studied river. In the TiO_2 vs. CaO diagram (Fig. 10b), once again the sediments plot in the field of HHCS. Higher concentration of CaO in sediments compared to LH lithologies, attracts similar argument as in the case of higher Na_2O compared to the LH rocks. Other than feldspars, the other major mineral in the sediments is mica (muscovite + biotite). Therefore, I have considered binary diagrams involving Fe, Mg and Ti (all constituents of mica group of minerals). In

FeO (T) vs. TiO_2 diagram (Fig. 10c), the sediments plot in the field of HHCS lithologies and also show a very tight correlation with it. In contrast, the LH lithologies plot in a separate field and exhibit a different trend line, and exhibit no specific variation in Fe corresponding to the variation in Ti. Similar trend is also observed in the diagram of FeO + MgO vs. TiO_2 (Fig. 10d).

In FeO/SiO_2 vs. Al_2O_3/SiO_2 diagram (Fig. 10e), the sediments plot between the various lithologies of HHCS rocks, indicating them to be produced as a result of mixing of these rocks. On the contrary, the sediments plot below the lower end of the spread for LH lithologies. LH rocks show varied and much higher concentration of FeO and Al_2O_3. It would require multiple recycling and great amount of fluvial reworking and sorting of LH rocks, to produce the chemistry similar to the studied sediments, which as inferred earlier is not true in the present case.

5.4. Comparison of REE

All the studied sediments exhibit similar chondrite normalized LREE fractionation and variable but low HREE fractionation, similar to the granodioritic rocks but with a very prominent negative Eu anomalies, which is larger than the average granodiorite or the UCC. This implies, that the sediments were derived from granitic to granodioritic source rocks. This was also inferred from the plots of La, Th, Sc and their ratios (Fig. 9a and b), and similarity of sediments with HHCS granite and gneisses (Fig. 10a–e). To further constrain the source, the UCC normalized REE patterns of sediments and the averages of the probable source rocks that include (i) schist and gneiss from the HHCS (Harris et al., 1992; Ayres and Harris, 1997), (ii) Cambro-Ordovician granites from middle and lower part of HHCS (Miller et al., 2001), and (iii) LH rocks (Rashid, 2005) have been compared.

The UCC normalized REE patterns of sediments from Bhagirathi (BG) and upper reaches of Alaknanda Rivers (AG) fall between that of the average UCC normalized patterns of HHCS schist and gneiss, and the HHCS Cambro-Ordovician granites (Fig. 11a). This suggests that these end member lithologies of HHCS could have acted as the source to the sediments. Schist and gneiss from HHCS appear to have relatively higher contribution to these sediments, as the pattern still remains HREE enriched. It is interesting to note that REE in the sediments of the Bhagirathi River (BG group), from different locations, although variable in their abundance, have similar UCC normalized REE pattern throughout its course. The REE pattern does not change even after the river has entered into and passes over Lesser Himalayan lithologies, which implies that the LH lithologies have little contribution to the sediment load of this river. Similarity of UCC normalized REE pattern along the entire traverse of this river also suggests that the relative proportion of REE holding phases have not been affected by fluvial processes, which is also indicated by the similarity of REE patterns of the bed load sediments and the suspended load from this

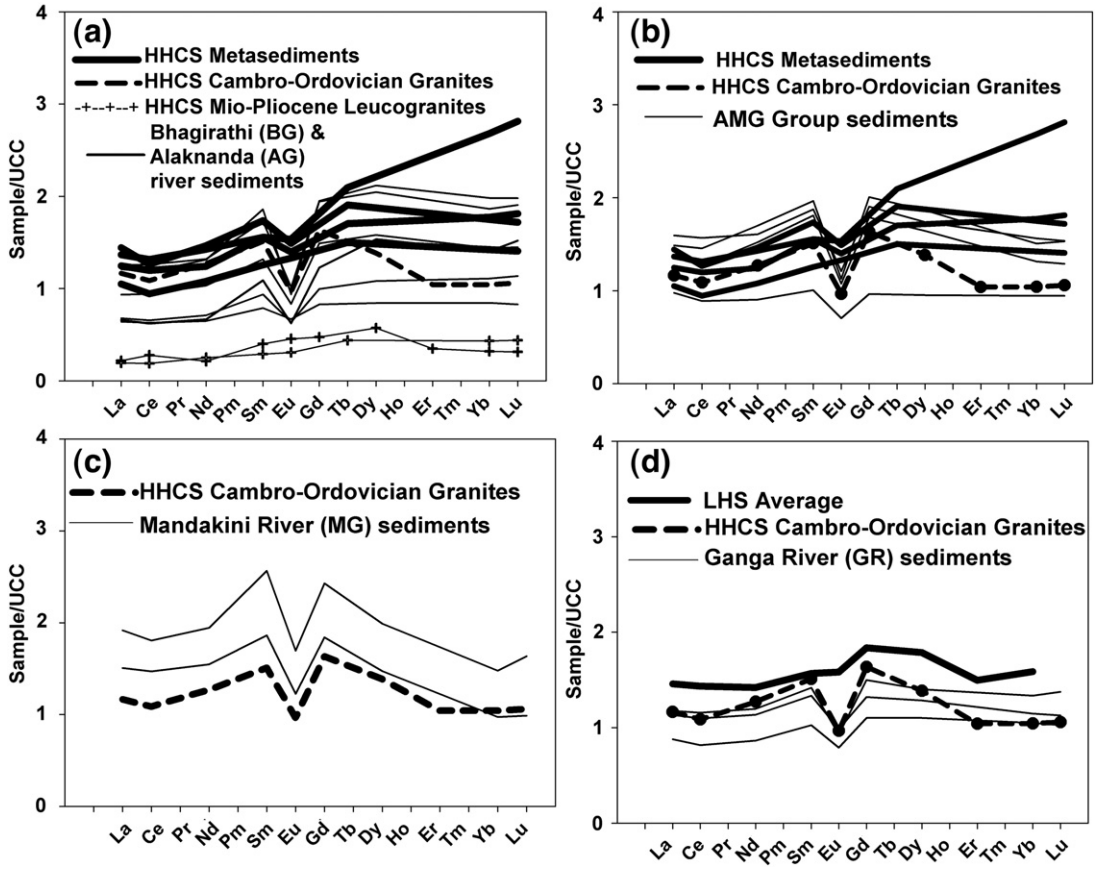

Fig. 11. UCC normalized REE pattern of sediment collected from (a) Bhagirathi river (BG group) and Alaknanda River (AG group) (b) Mandakini River (MG group) (c) Alaknanda and Mandakini Rivers in lower reaches (AMG group) and (d) the Ganga river (GR group) after Devprayag and before entering into the plains. Also plotted for comparison are the averages of probable source rocks from HHCS [metasediments and leucogranites (Harris et al., 1992; Ayres and Harris, 1997), Cambro-Ordovician granites (Miller et al., 2001)] and LHS (Rashid, 2005). Note that the sediments in (a) from Bhagirathi and Alaknanda rivers have a pattern similar to the Higher Himalayan metasediments and in (c) from Mandakini river have a pattern similar to Higher Himalayan Granites. The sediments after the confluence of the above tributaries i.e. from AMG group (b) and GR group (d) have a pattern intermediate between that of (a) and (c) and Metasediments and Granites from HHCS indicating that the sediments finally coming out of the Himalayas to the Gangetic plain are the mixture of the above two end members. Note that the UCC normalized pattern of LHS rocks has different patterns indicating little input from them to the sediments.

river (Fig. 6a). This also indicates that the REE bearing heavy mineral phases have attained hydrodynamic similarity in this river. Alaknanda River sediment in its lower reaches at Gauchar (A2), after its confluence with two major glacier fed tributaries namely Dhauli River and Pindar River, which probably originates in or cross the Cambrian/Ordovician granitic rocks, exhibits flattened UCC normalized REE pattern. There is a rotation of REE pattern compared to AG (Fig. 11a). This can be explained by modification of the pattern due to sediment input from Pindar River, which probably en route erodes Cambro/Ordovician granites having more fractionated REE patterns. The UCC normalized REE pattern of the Mandakini River sediments (MG) from upper reaches, exhibits prominent HREE depletion (Fig. 11c) and great amount of similarity with the average REE patterns of the Cambrian/Ordovician granites. This would suggest that these rocks have acted as the major source to the sediments in this part. Again in the lower reaches of this river the UCC normalized REE pattern of sediments is observed to flatten out (Fig. 11b), probably because of input from the HHCS gneiss and schist, which have HREE enriched patterns. Thus, it is observed that Alaknanda and Mandakini River sediments attain almost similar REE patterns, before their confluence at Rudraprayag.

After the confluence of Alaknanda River and the Mandakini River at Rudraprayag, the sediments (A3) maintain the REE pattern similar to that attained in the lower reaches of these rivers (Fig 11b). Higher abundance of REE observed in the sediment (A3) after the above confluence, is because of enrichment of heavy mineral, as indicated by higher Th and Zr content in it (Table 1). Relatively unaltered REE pattern of Alknanda River sediments through its passage over the LH after the confluence of the above tributaries, suggests that there is negligible contribution by the LH lithologies. This implies that the major source to the sediments of this river till it meets Bhagirathi River at Devprayag, is the HHCS lithologies. The two major tributaries, i.e. the Bhagirathi and the Alaknanda Rivers, meet at Devprayag and hereafter the mainstream river carry the name of the Ganga. Moving downstream from here, it is observed that the UCC normalized REE pattern of sediments collected at various locations (Fig. 1) from the Ganga River, show no further change in REE patterns and has attained a pattern intermediate between that of Alaknanda River and Bhagirathi River sediments before their confluence at Devprayag (Fig. 11d). This would suggest that there is no further addition from the LH lithologies and the pattern is result of mixing of Bhagirathi and Alaknanda river sediments. This suggests that the Ganga River sediments ultimately moving out of its hilly tract in the Himalayas into the Gangetic Plain had predominantly received sediments from various lithologies of HHCS; secondly its uniform REE patterns indicates that before entering the Gangetic Plain, the sediments have got completely homogenized as also exhibited by similarity of their major element chemistry; lastly, at this stage also there is not much effect of sorting on the sediments, as seen by the similarity of REE pattern of the bed load sediments from the Ganga River section and the suspended load from the same tract (Fig. 6e).

This implies that there is minimal input from the lithologies of Lesser Himalaya and the Siwaliks. This is found to be true on comparing the UCC normalized REE pattern of LH rocks, which is different from the sediments in that they show no Eu anomaly, and variable enrichment and depletion of LREE, MREE and HREE (Fig. 11d).

6. Conclusions

Major element chemistry and the lower values of CIA of all the sediments indicate that the source rocks supplying the detrital load to the Ganga River and its tributaries have not undergone significant chemical weathering. The low Al_2O_3/Na_2O (3.2–5.7) and K_2O/Na_2O (0.7–1.4) ratios of the studied sediments and their plot in the litharenite field in log (Na_2O/K_2O) vs. lopg($SiO_2/Al_2O_{3;}$) and log (SiO_2/Al_2O_3) vs. log (FeO/K_2O) diagrams and the lower values of CIA (45.–54.7) indicate that physical weathering and erosion rather than silicate weathering as the dominant process in the Himalayan catchment region of the Ganga River. All the sediments, collected right from their traverse in the Higher Himalaya through Lesser Himalaya and the Siwaliks, exhibit higher Na_2O, K_2O, CaO and silica. This and the higher ratios of La/Sc, Th/Sc and lower ratios of Co/Th suggest source rocks to be felsic in nature. Further the fractionated REE patterns and the marked negative Eu anomalies ($Eu/Eu^* = 0.27–0.53$) indicate highly differentiated source. A comparison among sediments and different source rock lithologies from HHCS and the LHS for their major elements in various bivariant plots clearly suggest that the HHCS rocks have acted as the predominant source rocks.

The REE patterns of the sediments from the primary tributaries are similar to their sources in the HHCS. The changes observed in their lower reaches and after their confluence are the result of mixing as indicated by the REE patterns in this part, which are intermediate between the REE patterns of the joining tributaries. This implies not much addition of sediments from en route catchment lithologies i.e. Lesser Himalayas and the Siwaliks Himalaya ; secondly the similarity of REE pattern between suspended and bed load indicates not much mineralogical sorting, which suggests that the sediments are simply the product of mechanically crushed rocks in which efficient mineral separation has not taken place.

The above conclusions hold significance as the estimate made on the solute input to the ocean water based solely on the studies limited to the catchment region of large rivers may be flawed. In an earlier paper (Singh, 2009) based on the sediments from the plains region of the Ganga River, we have shown that chemical weathering initiates only in this part.

Acknowledgments

This research was supported by a grant from the DST (No. DST/FTP/ES-40/2001) to PS and by DST FIST supported analytical facility at Department of Earth Sciences, Pondicherry University. I am grateful to David Rickard and Roberta Rudnick, the editors, for their comments and suggestions and to anonymous reviewers for their constructive reviews. The paper benefited from discussions with my colleagues Subhadip Bhadra and Rajneesh Bhutani during the revision.

Appendix A

Table 1A
Results of analysis of reference standards by ICP-AES and WD-XRF.

Elements analyzed by ICP-AES				
	Standard BHVO-1	BHVO-1	Rsd %	Dev. % with respect to mean
	reported values	mean analyzed value	$n=6$	
TiO_2	2.69	2.74	0.71%	−1.86
Al_2O_3	13.7	13.66	0.72%	0.29
FeO	12.27	12.3	0.42%	−0.24
MgO	7.2	7.15	0.25%	0.69
MnO	0.17	0.17	0.97%	0.00
CaO	11.32	11.52	0.61%	−1.77
Na_2O	2.24	2.23	0.89%	0.45
K_2O	0.52	0.53	0.97%	−1.92
P_2O_5	0.27	0.269	1.36%	0.37
Ba	139	146	1.07%	−5.04
Sr	403	391	0.93%	2.98
Ni	121	125	0.83%	−3.31
Cr	289	283	0.73%	2.08
Y	28	29	1.67%	−3.57

Table 1A (*continued*)

Elements analyzed by ICP-AES

	Standard RGM-1	RGM-1	Rsd %	Dev. % with respect to mean
	reported values	mean analyzed value	$n=4$	
La	24	24.8	1.43	−3.33
Ce	47	48.01	1.2	−2.15
Nd	19	19.12	0.87	−0.63
Sm	4.3	4.39	0.86	−2.09
Eu	0.66	0.68	0.54	−3.03
Gd	3.7	3.78	0.86	−2.16
Dy	4.08	4.17	1.06	−2.21
Yb	2.6	2.64	0.98	−1.54
Lu	0.41	0.42	1.01	−2.44

Elements analyzed by WD-XRF

	Standard SO-1	SO-1	Rsd %	Dev. % with respect to mean
	reported values	mean analyzed value		
Th	12.4	11	2.5	11.2
Sc	17.7	16.17	1.62	8.6
Co	29	32.5	2.15	−12
U	1.71	2	0.5	−16
Zr	84	82	2.5	2.3

References

Ahmad, T., Harris, N., Bickle, M., Chapman, H., Bunbury, J., Prince, C., 2000. Isotopic constraints on the structural relationships between the Lesser Himalayan Series and the High Himalayan Crystalline Series, Garhwal Himalaya. GSA Bulletin 112, 467–477.

Ayres, M., Harris, N., 1997. REE fractionation and Nd-isotope disequilibrium during crustal anatexis; constraints from Himalayan leucogranites. Chemical Geology 139, 249–269.

Bauluz, B., Mayayo, M.J., Fernandez-Nieto, C., Lopez, J.M.G., 2000. Geochemistry of Precambrian and Paleozoic siliciclastic rocks from the Iberian Range (NE Spain): implications for source area weathering, sorting, provenance and tectonic setting. Chemical Geology 168, 135–150.

Berner, R.A., 1992. Weathering, plants, and the long term carbon cycle:. Geochimica et Cosmochimica Acta 56, 3225–3231.

Berner, R.A., 1995. In: White, A.F., Brantley, S.L. (Eds.), Chemical weathering and its effect on atmospheric CO_2 and climate. Chemical Weathering Rates of Silicate Minerals, vol. 31. Mineralogical Society of America, pp. 565–583.

Bhatia, M.R., 1985. Rare earth geochemistry of Australian Paleozoic greywackes and mudrocks: provenance and tectonic control. Sedimentary Geology 45, 97–113.

Bhatia, M.R., Crook, K.A.W., 1986. Trace element characteristics of greywackes and tectonic setting discrimination of sedimentary basins. Contributions to Mineralogy and Petrology 92, 181–193.

Bickle, M.J., Harris, N.B.W., Bunbury, J., Chapman, H.J., Fairchild, I.J., Ahmad, T., 2001. Controls on the 87Sr/86Sr of carbonates in the Garhwal Himalaya, headwaters of the Ganges. Journal of Geology 109, 737–753.

Bickle, M.J., Bunbury, J., Chapman, H.J., Harris, N.B.W., Fairchild, I.J., Ahmad, T., 2003. Fluxes of Sr into the headwaters of the Ganges. Geochimica et Cosmochimica Acta 67, 2567–2584.

Bluth, G.J.S., Kump, L.R., 1994. Lithologic and climatologic controls of river chemistry. Geochimica et Cosmochimica Acta 58, 2341–2359.

Cerling, T.E., Harris, J.M., MacFadden, B.J., Leakey, M.G., Quade, J., Eisenmann, V., Ehleringer, J.R., 1997. Global vegetation change through the Miocene/Pliocene boundary. Nature 389, 153–158.

Chakrapani, G.J., 2005. Major and trace element geochemistry in upper Ganga river in the Himalayas, India. Environmental Geology 48, 189–201.

Condie, K.C., 1993. Chemical composition and evolution of the upper continental crust: contrasting results from surface samples and shales. Chemical Geology 104, 1–37.

Derry, L.A., France-Lanord, C., 1996. Neogene Himalayan weathering history and river 87Sr/86Sr: impact on marine Sr record. Earth and Planetary Science Letters 142, 59–74.

Drever, J.I., Zobrist, J., 1992. Chemical weathering of silicate rocks as a function of elevation in the southern Swiss Alps. Geochimica et Cosmochimica Acta 56, 3209–3216.

Dupré, Bernard, Dessert, Céline, Oliva, Priscia, Goddéris, Yves, Viers, Jérôme, François, Louis, Millot, Romain, Gaillardet, Jérôme, 2003. Rivers, chemical weathering and Earth's climate. Comptes Rendus Geosciences 335, 1141–1160.

Edmond, J.M., 1992. Himalayan tectonics, weathering processes, and the strontium isotope record in marine limestones. Science 258, 1594–1597.

Frallick, P.N., Kronberg, B.I., 1997. Geochemical discrimination of clastic sedimentary rock sources. Sedimentary Geology 113, 111–124.

Gale, J.G., Hoare, P.G., 1991. The physical composition and analysis of regolith materials, in Quaternary Sediments: Petrographic Methods for the Study of Unlithified Rocks: New York, Belhaven Press, pp. 87–94.

Galy, A., France-Lanord, C., 2001. Higher erosion rates in the Himalaya: geochemical constraints on riverine fluxes. Geology 29, 23–26.

Galy, A., France-Lanord, C., Derry, L.A., 1999. The strontium isotopic budget of Himalayan Rivers in Nepal and Bangladesh. Geochimica et Cosmochimica Acta 63, 1905–1925.

Gannser, A., 1964. Geology of the Himalayas. Interscience, London, p. 289.

Govindraju, K., 1994. Compilation of working values and description for 383 geostandards. Geostandards Newsletter 18, 1–158.

Harris, N.W.B., Gravestock, P., Inger, S., 1992. Ion-microprobe determination of trace element concentrations in garnets from anatectic assemblages. Chemical Geology 100, 41–49.

Harris, N., Bickle, M., Chapman, H., Fairchild, I., Bunbury, J., 1998. The significance of Himalayan rivers for silicate weathering rates: evidence from the Bhote Kosi tributary. Chemical Geology 144, 205–220.

Herron, M.M., 1988. Geochemical classification of terrigenous sands and shales from core or log data. Journal of Sedimentary Petrology 58, 820–829.

Jacobson, A.D., Blum, J.D., 2003. Relationship between mechanical erosion and atmospheric CO_2 consumption of the New Zealand Southern Alps. Geology 31, 865–868.

Jacobson, A.D., Blum, J.D., Walter, L.M., 2002. Reconciling the elemental and Sr isotope composition of Himalayan weathering fluxes: insights from the carbonate geochemistry of stream waters. Geochimica et Cosmochimica Acta 66 (19), 3417–3429.

Johnson, M.R.W., Oliver, G.J.H., 1990. Pre-collisional and post-collisional thermal events in the Himalaya. Geology 18, 753–756.

Krishnaswami, S., Trivedi, J.R., Sarin, M.M., Ramesh, R., Sharma, K.K., 1992. Strontium isotopes and rubidium in the Ganga–Brahmaputra river system: weathering in the Himalaya, fluxes to the Bay of Bengal and contributions to the evolution of oceanic 87Sr/86Sr. Earth and Planetary Science Letters 109, 243–253.

Krishnaswami, S., Singh, S.K., Dalai, T.K., 1999. Silicate weathering in the Himalayas: role in contributing to major ions and radiogenic Sr to the Bay of Bengal. In: Somayajulu, B.L.K. (Ed.), Ocean Science, trends and future directions. Indian National Science Academy and Akademi Book International, New Delhi, pp. 23–51.

McDonough, W.F., Sun, S.S., 1995. The composition of the earth. Chemical Geology 120, 223–253.

McLennan, S.M., Taylor, S.R., 1991. Sedimentary rocks and crustal evolution: tectonic setting and secular trends. Journal of Geology 99, 1–21.

McLennan, S.M., Hemming, S., McDennial, D.K., Hanson, G.N., 1993. Geochemical approaches to sedimentation, provenance and tectonics. Geological Society of America Special Paper 284, 21–40.

Miller, C., Thoni, M., Frank, W., Grasemann, B., Klotzli, U., Guntil, P., Draganits, E., 2001. The early Palaeozoic magmatic event in the northwest Himalaya, India: source, tectonic setting and age of emplacement. Geological Magazine 138 (3), 237–251.

Nesbitt, H.W., Young, G.M., 1984. Prediction of some weathering trends of plutonic and volcanic rocks based on thermodynamic and kinetic consideration. Geochimica et Cosmochimica Acta 48, 1523–1534.

Nesbitt, H.W., Young, G.M., 1989. Formation and diagenesis of weathering profiles. Journal of Geology 97, 129–147.

Palmer, M.R., Edmond, J.M., 1989. The Sr isotope budget of the modern ocean. Earth and Planetary Science Letters 92, 11–26.

Palmer, M.R., Edmond, J.M., 1992. Controls over the Sr isotope composition of river water. Geochimica et Cosmochimica Acta 56, 2099–2111.

Pettijohn, F.J., Potter, P.E., Siever, R., 1972. Sand and sandstones. Spriger, New York.

Quade, J., Cater, J.M.L., Ojha, T.P., Adam, J., Harrison, T.M., 1995. Late Miocene environmental change in Nepal and the northern Indian subcontinent: stable isotopic evidence from paleosols. GSA Bulletin 107 (12), 1381–1397.

Quade, J., Roe, L., DeCelles, P.G., Ojha, T.P., 1997. The late Neogene 87Sr/86Sr record of lowland Himalayan rivers. Science 276, 1828–1831.

Rashid, S.A., 2005. The geochemistry of Mesoproterozoic clastic sedimentary rocks from the Rautgara Formation, Kumaun Lesser Himalaya: implications for provenance, mineralogical control and weathering. Current Science 88 (11), 1832–1836.

Raymo, M.E., Ruddiman, W.F., 1992. Tectonic forcing of Late Cenozoic climate. Nature 359, 117–122.

Raymo, M.E., Ruddiman, W.F., Froelich, P.N., 1988. Influence of late Cenozoic mountain building on ocean geochemical cycles. Geology 16, 649–653.

Retallack, G.J., 1991. Miocene paleosols and ape habitats of Pakistan and Kenya. Oxford University Press, New York.

Retallack, G.J., 2004. Late Miocene climate and life on land in Oregon within a context of Neogene global change. Palaeogeography, Palaeoclimatology, Palaeoecology 214, 97–123.

Retallack, G.J., 2009. Cenozoic cooling and grassland expansion in Oregon and Washington. PaleoBios 28 (3), 89–113.

Richards, Andy, Tom, Argles, Harris, Nigel, Parrish, Randy, Ahmad, Talat, Darbyshire, Fiona, Dragantis, Erich, 2005. Himalayan architecture constrained by isotopic tracers from clastic sediments. Earth and Planetary Science Letters 236, 773–796.

Richter, F.M., Rowley, D.B., DePaolo, D.J., 1992. Sr isotope evolution of sea water. The role of tectonics. Earth and Planetary Science Letters 109, 11–23.

Saini, N.K., Mukherjee, P.K., Rathi, M.S., Khanna, P.P., Purohit, K.K., 2002. Trace element estimation in soils: An appraisal of ED-XRF technique using group analysis scheme. Journal of Trace and Microprobe Techniques 20 (4), 539–551.

Searle, M.P., Noble, S.R., Hurford, A.J., Rex, D.C., 1999. Age of crustal melting, emplacement and exhumation history of Shivling leucogranite, Garhwal Himalaya. Geological Magazine 136 (5), 513–525.

Shapiro, L., Brannock, W.W., 1962. Rapid analysis of silicate, carbonate, and phosphate rocks. United States Geological Survey Bulletin 1144A, 1–56.

Singh, P., 2009. Major, trace and REE geochemistry of the Ganga River sediments: influence of provenance and sedimentary processes. Chemical Geology 266, 251–264.

Singh, P., Rajamani, V., 2001. REE Geochemistry of recent clastic sediments from the Kaveri floodplains, southern India: implication to source area weathering and sedimentary processes. Geochimica et Cosmochimica Acta 65 (18), 3093–3108.
Stallard, R.F., Edmond, J.M., 1983. Geochemistry of the Amazon, the influence of geology and weathering environment on the dissolved load. Journal of Geophysical Research 88.967, 1–9688.
Stallard, R.F., Edmond, J.M., 1987. Geochemistry of the Amazon, weathering chemistry and limits to dissolved inputs. Journal of Geophysical Research 92, 8293–8302.
Taylor, S.R., McLennan, S.M., 1985. The Continental Crust: Its Composition and Evolution. Blackwell, Oxford. 312 pp.
Valdiya, K.S., 1980. Geology of the Kumaun Lesser Himalayas. Wadia Inst. Himalayan Geology. The Himachal times press, Dehradun, India.
Valdiya, K.S., 1995. Proterozoic sedimentation and Pan-African geodynamic development of the Himalaya. Precambrian Research 74, 35–55.
Vieizer, J., 1989. Strontium isotopes in sea water through time. Annual Review of Earth and Planetary Sciences 17, 141–168.